

---

## Reviewer 1

### General Comments:

This study examines the domestic and foreign influence of anthropogenic emissions on ozone over China using the GEOS-Chem model and two methods of identifying contributions, a “zero-out” approach and a tagging approach (which seems to be missing from the manuscript). After first validating the model’s capabilities against surface and ozonesonde observations, they proceed to characterize the spatial influence (horizontally and vertically) of natural, background, foreign anthropogenic and domestic anthropogenic emissions on ozone over China.

Much of the analysis in this manuscript contains significant insights into the ozone chemistry over China and the impact of foreign and domestic emissions on tropospheric ozone. This manuscript could be a valuable contribution to ACP and to our understanding of ozone attribution over China, but there are several major items that need to be addressed before I can recommend publication. I discuss two major issues below, and conclude with technical comments.

We thank the referee for helpful comments. We respond to each comment below. The referee comments are shown in red. Our replies are shown in black.

### Specific Comments:

First, this study examines a single 3-month period (spring) in 2008 and draws extensive conclusions based on this period. The nature of emissions, ozone chemistry, meteorology, and atmospheric transport make it difficult to believe in the robustness of results drawn from such a short period without some characterization of the trends, variability, and uniqueness/non-uniqueness of this particular spring in 2008. While the authors point out the reasons for selecting this time period (L102-107), and while they mention some of these issues (e.g. NO<sub>x</sub> trends in L282-285, differences in emissions and meteorology in L311-312), I do not believe there is a sufficient demonstration of the robustness of their results, and there are many questions that need to be addressed. Are the results drawn throughout Sections 4 and 5 robust for different years, or are they sensitive to chemical and meteorological variability and thereby vary from year-to-year? How much do they vary? Where does the spring of 2008 fit into the bigger ozone/chemistry/meteorology context over China?

I feel that either: (1) additional simulations including at least one additional year are required to demonstrate the simulated variability of ozone over China and the robustness of these results; or (2) the manuscript requires additional literature reviews and a careful description of the ozone variability over China as a demonstration of the robustness of the results. In L247-253 the authors discuss an additional year of simulation, which could certainly provide some of this temporal variability context. Some of the publications below could provide some of this context and reasons why 3-months is not long enough to draw strong conclusions, especially with regards to ozone:

Xu, X., Lin, W., Wang, T., Yan, P., Tang, J., Meng, Z., and Wang, Y.: Long-term trend of surface ozone at a regional background station in eastern China 1991–2006: enhanced

---

variability, *Atmos. Chem. Phys.*, 8, 2595-2607, <https://doi.org/10.5194/acp-8-2595-2008>, 2008.

Jin, X., and T. Holloway, Spatial and temporal variability of ozone sensitivity over China observed from the Ozone Monitoring Instrument, *J. Geophys. Res. Atmos.*, 120, 7229–7246, doi:10.1002/2015JD023250, 2015

W.N. Wang, T.H. Cheng, X.F. Gu, H. Chen, H. Guo, Y. Wang, F.W. Bao, S.Y. Shi, B.R. Xu, X. Zuo, C. Meng, X.C. Zhang, Assessing spatial and temporal patterns of observed ground-level ozone in China, *Sci. Rep.*, 7 (1), p. 3651, 10.1038/s41598-017-03929-w, 2017.

Garcia-Menendez, F., Monier, E., and Selin, N. E.: The role of natural variability in projections of climate change impacts on U.S. ozone pollution, *Geophys. Res. Lett.*, 44, 2911–2921, 2017.

Brown-Steiner, B., Selin, N. E., Prinn, R. G., Monier, E., Tilmes, S., Emmons, L., and Garcia-Menendez, F.: Maximizing Ozone Signals Among Chemical, Meteorological, and Climatological Variability, *Atmos. Chem. Phys. Discuss.*, <https://doi.org/10.5194/acp-2017-954>, in review, 2017.

Thanks for your suggestion.

As in the newly added Sect. 4.3 (Line 492-516), previous studies have shown notable interannual variability in surface ozone over China driven by changes in precursor emissions and meteorology (Xu et al., 2008; Jin et al., 2015; Wang et al., 2017). To test how the interannual variability of meteorology and emissions would affect our source attribution findings, we have repeated all zero-out runs for spring 2012, the latest year when the GEOS-5 meteorological fields are available. Emissions for 2012 were adopted from the Community Emissions Data System (CEDS) inventory (Hoesly et al., 2018); 2012 is also the latest year the CEDS emissions for China are adjusted by the MEIC inventory. Table A1 shows the anthropogenic emissions in the two years. All zero-out simulation results in 2012 underwent the same linear weighting adjustment as for those in 2008. Figure A1d–f show the results for domestic versus foreign contributed ozone in spring 2012, as compared to the results for spring 2008 (adopted from Fig. 9a–c in the revised paper). In absolute terms, Chinese contributed ozone are similar between 2008 and 2012 (comparing Fig. A1a and d), reflecting the slight changes in domestic precursor emissions (Table A1). From 2008 to 2012, the absolute foreign contributed ozone increase along the southern boarder due to much enhanced emissions in South-East Asia and South Asia. The absolute foreign contributions decrease over the north and south, reflecting the net effect of changes in European and North American emissions (within 20% for both NO<sub>x</sub> and NMVOC), increased emissions in Rest of Asia, and changes in meteorology. In relative terms (Fig. A1c and f), the percentage foreign anthropogenic contributions to total anthropogenic ozone decrease from 2008 to 2012 over southern China. Nonetheless, in both years the percentage foreign contributions exceed 50% over western China and are 5–40% over southern China. Therefore our general finding that both foreign and domestic contributions to Chinese anthropogenic ozone are important holds true for these two years.

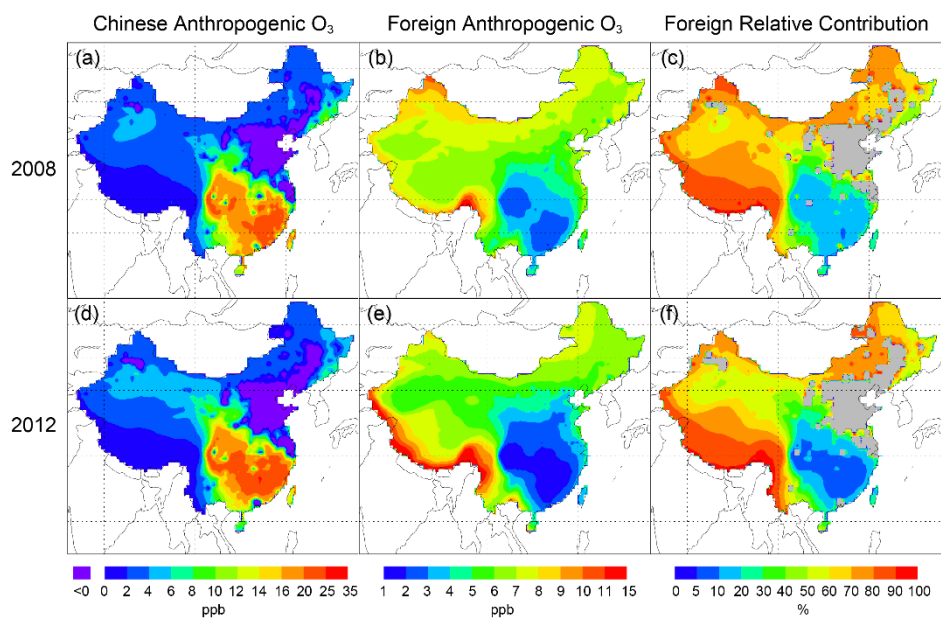


Figure A1. Spatial distribution of springtime daily mean surface ozone over China contributed by (a) domestic and (b) foreign anthropogenic emissions in 2008. (c) Percentage contribution of foreign anthropogenic emissions to total anthropogenic ozone in 2008; areas with negative Chinese contributions (due to NO<sub>x</sub> titration) are marked in grey. (d–f) similar to (a–c) but for results of 2012. The linear weighting adjustment is applied to derive all results. Please note that the color scales are different between (a, d) and (b, e).

Table A1. Springtime anthropogenic emissions of NO<sub>x</sub>, CO and NMVOC in 2008 and 2012 in each source region defined in Fig. 1.

	2008	China	Japan and Korea	South-East Asia	South Asia	Rest of Asia	Europe	North America	Rest of world
NO <sub>x</sub> (TgN)		2.0	0.3	0.4	0.4	0.7	1.2	1.3	1.0
CO (Tg)		42.3	1.7	10.9	16.7	10.0	12.5	17.7	25.5
NMVOC (TgC)		2.9	0.2	1.3	1.3	1.1	1.1	2.1	1.9
	2012								
NO <sub>x</sub> (TgN)		2.2	0.3	0.6	1.3	1.0	1.0	1.1	1.5
CO (Tg)		39.2	2.4	15.4	21.3	8.9	7.9	13.1	38.0
NMVOC (TgC)		3.0	0.2	3.0	2.4	2.3	1.2	1.8	6.8

Reference:

Hoesly, R. M., Smith, S. J., Feng, L., Klimont, Z., Janssens-Maenhout, G., Pitkanen, T., Seibert, J. J., Vu, L., Andres, R. J., Bolt, R. M., Bond, T. C., Dawidowski, L., Kholod, N., Kurokawa, J.-I., Li, M., Liu, L., Lu, Z., Moura, M. C. P., O'Rourke, P. R., and Zhang, Q.: Historical (1750–2014) anthropogenic emissions of reactive gases and aerosols from the Community Emissions Data System (CEDS), *Geosci. Model Dev.*, 11, 369-408, <https://doi.org/10.5194/gmd-11-369-2018>, 2018

Second, the manuscript at times leaves out critical information or does not sufficiently describe methods, definitions, and figures. While this manuscript contains many valuable results, there were several moments where I didn't feel there was enough information provided to understand what was done, or why it was done, and times when I had to search for descriptions and/or infer some explanations on my own. The following list summarizes areas and issues that need to be addressed and revised:

(1) The authors state that they combine zero-out simulations with tagged ozone simulations (and the tagged ozone simulations are mentioned in Table 2 and on L110, L114, and L183-187), but nowhere throughout the rest of the manuscript are the tagged ozone results described or shown. Were they not used? Where are the descriptions of these results?

As mentioned in our original manuscript (Line 84–85), ozone over China attributed to anthropogenic emissions of an emission source region can be produced both within the domain of that source region and outside the domain due to the outflow of ozone precursors. The zero-out simulations provide the total transboundary ozone due to emissions of a source region. The tagged ozone approach quantifies the ozone produced in any designated region, with no information about whether the associated precursors are emitted in that region or are transported from somewhere else.

We combined tagged ozone simulations with the zero-out method to quantify the contribution of ozone over China attributed to anthropogenic emissions of each source region produced *within* and *outside* that source region, respectively. Results combining

tagged ozone simulations and zero-out simulations are shown in Sect. 5 and Fig. 13c (Fig. 11c in the original manuscript).

For further explanation, here we take ozone over China attributed to European anthropogenic emissions as an example. The tagged ozone approach quantifies ozone over China produced in any designated region (due to global emissions), which is defined as an artificial “tracer” in the tagged simulation. We defined 10 producing regions and thus 10 artificial tracers in tagged simulations, including eight tropospheric above-land domains (China, Europe, etc.), tropospheric above-ocean domain, and the stratosphere. To complement the full-chemistry control case (CTL), we ran the tagged simulation to calculate the contributions from these 10 producing domains (and 10 artificial tracers) (T\_CTL). For the zero-European-anthropogenic-emissions case (xEU, a zero-out simulation), we did a similar calculation (T\_xEU). Thus, the difference between CTL and xEU gave the total ozone due to European anthropogenic emissions, and the difference between T\_CTL and T\_xEU gave the concentration of ozone produced over each of these 10 producing domains due to European anthropogenic emissions. To account for the effect of chemical nonlinearity in these attribution analyses, we further applied a weighting to these results.

We have revised the introduction of the new Fig. 13c (the old Fig. 11c) (Line 538-542) as “Figure 13c further separates the portion of ozone produced within each source region’s territory from the portion produced outside of that source region; results here were derived from a combination of zero-out simulations (e.g., CTL and xEU) and tagged simulations (e.g., T\_CTL and T\_xEU).”

(2) A linear weighting method is used to adjust the ozone attribution results, and is described on L188-195, but the description is insufficient. I am not familiar with this method, so I do not fully understand what Equation 1 means, and tracing back to the Li et al. (2016a) citation brings me to a ‘normalized marginal method’ used for radiative forcing attribution, not ozone attribution. It is not clear to me where the precise formulation of Equation 1 came from, what it does, what impact the adjustment has on the results, or why it was selected.

Ozone production is nonlinearly dependent on its precursors. Thus, the sum of natural ozone and anthropogenic ozone due to each emission source region calculated from zero-out simulations is not equal to ozone concentration calculated in the control run (CTL). Considering uncertainties induced by emission perturbation methods, we used a linear weighting method to adjust ozone concentration attributed to different sources, ensuring that the sum of natural ozone and anthropogenic ozone in zero-out simulations is equal to amount of ozone simulated in CTL.

As clarified in the revised manuscript, here is an example to adjust Chinese contribution to ozone over China using the linear weighting approach. Equation A1 calculates the fractional Chinese contribution ( $\alpha$ ) to the sum of ozone from individual anthropogenic source regions and from natural sources; the simulations involved are all full-chemistry runs (CTL, xCH, xEU, ..., xANTH). Equation A2 applies the fractional contribution  $\alpha$  to the total ozone in CTL to obtain the final adjusted Chinese contribution. These equations are used in the revised manuscript for better clarity; they are simply a transformed version of Eq. 1 in the original manuscript.

Similar adjustments were applied to other source regions, such that all results shown in our original manuscript are for “adjusted” ozone attribution through this linear weighting approach.

As shown in our revised manuscript Line 216–218, “A similar approach was used by Li et al. (2016a) to estimate the contribution of China to global radiative forcing, although in their study 20% (instead of 100%) of emissions over individual emission source regions

are removed in the sensitivity simulations.”

$$\alpha = \frac{\text{Con(CTL)} - \text{Con(xCH)}}{\sum_{i=1}^8 [\text{Con(CTL)} - \text{Con(Ci)}] + \text{Con(xANTH)}} \quad (\text{A1})$$

$$C_{\text{CH}} = \alpha \times \text{Con(CTL)} = \frac{\text{Con(CTL)} - \text{Con(xCH)}}{\sum_{i=1}^8 [\text{Con(CTL)} - \text{Con(Ci)}] + \text{Con(xANTH)}} \times \text{Con(CTL)} \quad (\text{A2})$$

(3) Many of the comparisons to observations compared the simulated spring of 2008 with other years (e.g. L281-285, L297-298, L311-312), and given the variability in ozone, chemistry, and meteorology (see above), I'm not sure these are wholly valid comparisons, especially without the broader temporal context of ozone over China. Some sort of quantification of measurement-model uncertainty and sensitivity to the time periods compared needs to be included.

In our study, in order to use as many observations to constrain model ozone as possible, we included a suite of measurement data in spring 2008 and in other years. For surface ozone, we focused on the comparison with observations in 2008 that are temporally consistent with our simulation; we showed the day-to-day variation at those sites. We extended the comparison to surface measurements in other years, in order to give a sense of how model ozone is situated in the general ozone pollution phenomena, as also explained in the revised manuscript. For vertical profiles, we have tried our best to match the time of observations and model simulations. For comparison with MOZAIC from earlier years, we are more concerned with the general vertical shape, given the trends and interannual variability. Long-term observations indicate strong ozone growth over China due to changes in domestic precursor emissions (e.g., Wang et al., 2009; Xia et al., 2016). This growth is consistent with our results that model ozone in 2008 are generally higher than observations in earlier years, although the vertical shape is captured fairly well.

In explaining Table 4, we have revised the text Line 307–315 as follows:

“The model has a large overestimate by 48% at the Hok Tsui coastal rural site in Hong Kong (36.0 versus 53.4 ppb), although the times are different (2008 versus 1994–2007). Wang et al. (2009) shows that the springtime ozone concentration at this site increased from 1994 to 2007 at a rate of 0.41 ppb/yr, partly explaining this difference. The remaining difference may reflect that the model resolution is not able to represent the complex local terrain and land-sea contrast at this site. The model overestimates ozone at an urban site in Nanjing by 16%, although the observations were made in 2000–2002 when Chinese anthropogenic emissions of NO<sub>x</sub> were only about half of those in 2008 (Xia et al., 2016).”

In explaining the comparison with MOZIC profiles, we revised the text Line 339–342 as follows:

“The model overestimates ozone in the middle and upper troposphere over Shanghai, with larger biases at higher altitudes, likely indicating too strong STE. Other causes may include differences in meteorology and growth in emissions between 2000–2005 and 2008, as discussed for the surface ozone in Sect. 3.1.”

(4) The authors define ‘natural ozone’ on L353, ‘background ozone’ on L363, ‘domestic anthropogenic ozone’ on L369, but do not define ‘foreign anthropogenic ozone,’ leaving

it to the reader to infer a definition. Also, I'm not sure that 'natural ozone' is an accurate description of what is described, as humans have influenced atmospheric chemistry beyond just anthropogenic emissions, perhaps 'non-anthropogenic ozone' instead?

Anthropogenic ozone of each foreign region is defined as the difference between the base simulation CTL and each zero-out simulation with no anthropogenic emissions in that foreign region (e.g., xEU), followed by a linear weighting adjustment to account for chemical nonlinearly (Eq. 1 and 2). The total foreign anthropogenic ozone is determined by adding each foreign region's anthropogenic ozone contribution together.

We agree that human behaviors have also affected the climate and other processes that in turn will affect the chemical environment. We used the term "natural ozone" to be consistent with the literature in this area (e.g., Wang et al., 2011).

(5) Figure 10 should include a plot of the regions where Chinese emissions are the dominant contributor. Figure 10b shows that on average, China contributes ~50% to surface ozone, and it's clear from Figure 8 that Chinese emissions dominate southeastern China's ozone. I'm not sure it's worthwhile then to point out the dominant foreign contribution to surface ozone over regions where Chinese emissions are dominant, especially when the foreign contribution is so low (Figure 8b, c). On its own, Figure 1a is an incomplete representation.

Thanks for your suggestion. The regions where Chinese emissions are the dominant contributor are shown in Figure A2a. We have also added this plot into the new Fig. 11 (old Fig. 10).

We have added in the revised manuscript Line 448–453 that:

"Figure 11a shows whether Chinese or foreign anthropogenic contributions are higher at individual locations. Chinese anthropogenic contributions are higher than foreign contributions over southern China and parts of northern China. However, foreign anthropogenic contributions exceed domestic contributions over western China and most of the north, including the populated North China Plain. Over western China, foreign emissions contribute 70–90% of the total anthropogenic ozone (Fig. 9c)."

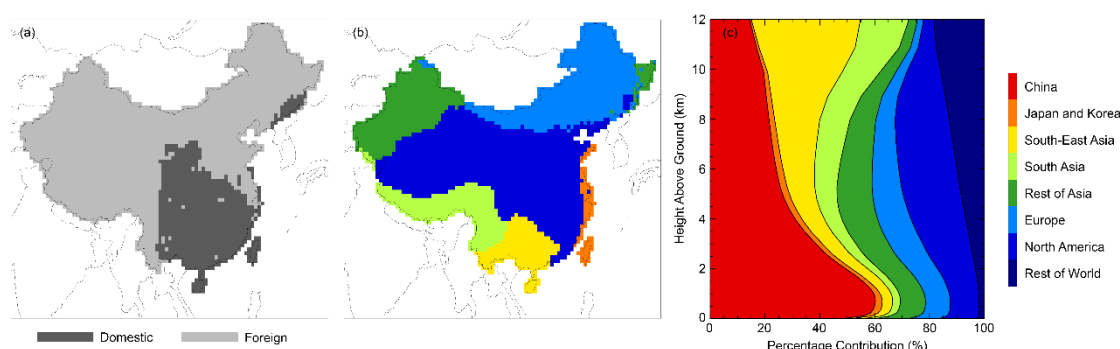


Figure A2. (a) Indication of the largest anthropogenic contributor (domestic versus foreign) to surface ozone at individual locations of China. (b) Indication of the largest foreign anthropogenic contributor to surface ozone at individual locations of China. (c) Vertical distribution of percentage contribution of each region to total anthropogenic ozone over China.

(6) Figure 11 is hard to parse, and given the large spatial heterogeneity shown in the other Figures, it is not clear to me that a single vertical plot averaging all of China provides

valuable information, or if it muddles interesting information through the averaging. This also applies to Figure 10b. Perhaps split these vertical profiles up into regions dominated by domestic and foreign contributions? Or perhaps apply some population weighing? In addition, Figure 11a should also include total ozone and a comparison should be made of total ozone (from the CTL run) and the sum of natural ozone, domestic anthropogenic ozone, and foreign anthropogenic ozone. It's not clear that these will match up, but it would speak to the non-linearity of the ozone simulations and contribution sensitivity simulations. Finally, I had difficulty in understanding Figure 11c as I initially assumed that Figure 11c was just a reformulation of Figure 11b in percentages rather than ppbv. The caption of the figure and the description on L484-485 are not clear, and as there is no description of how they arrived at this calculation, I'm unsure precisely what Figure 11c plots. The analysis summarized in these plots is interesting, but as is I have more questions that could be answered by subdividing these plots.

We have added a new figure (Fig. 14, also shown here as Fig. A3) with two sets of plots, one for the average over regions where Chinese anthropogenic emissions contribute more surface ozone than total foreign anthropogenic emissions (i.e., southern China), and the other for the regions where foreign anthropogenic emissions dominate.

As also discussed in the end of revised Sect. 5, even over areas where domestic contributions to near-surface ozone exceed total foreign contributions, the regional average ozone contributed by foreign emissions exceeds those contributed by domestic emissions above 3.5 km (Fig. A3a). Figure A3c and d further shows that the (relative) vertical shape of regional average ozone contributed by each foreign source region is similar to the shape of China averaged results in Fig. 13b, although the absolute values (in ppb) are different.

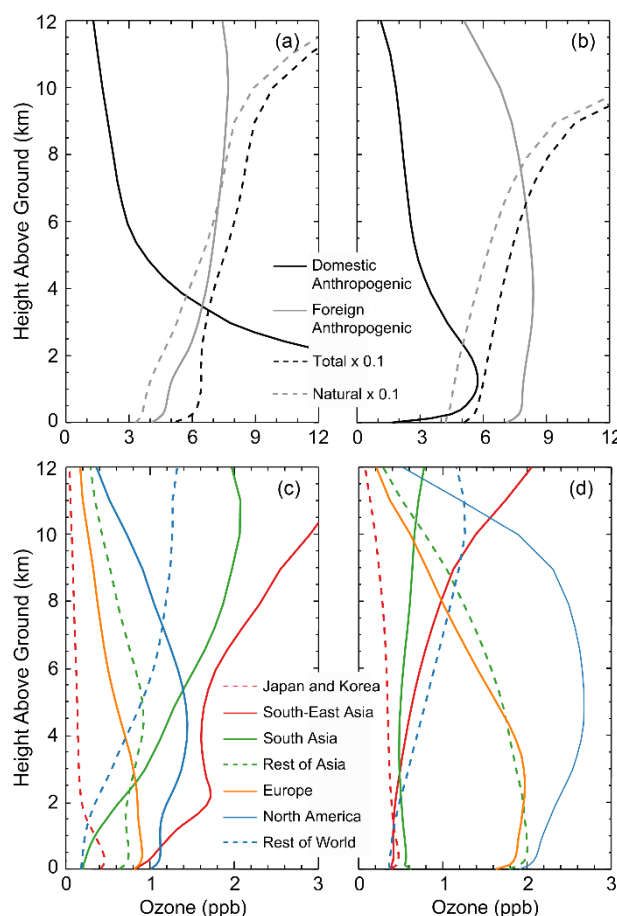


Figure A3. (a) Vertical distribution of regional average daily mean ozone contributed by domestic anthropogenic emissions, foreign anthropogenic emissions, natural sources (scaled by 0.1) and total sources (scaled by 0.1) over regions where Chinese anthropogenic emissions contribute more surface ozone than total foreign anthropogenic

emissions. (c) Contribution by anthropogenic emissions of each foreign source region over regions where Chinese anthropogenic emissions contribute more surface ozone than total foreign anthropogenic emissions. (b, d) similar to (a, c) but for regional average daily mean ozone over regions where foreign anthropogenic emissions dominate. The linear weighting adjustment is applied to derive all results.

We have added total ozone from CTL into the new Fig. 13a (old Fig. 11a, also shown here as Fig. A4a). We also added a new plot in the revised manuscript (new Fig. 2b, also shown here as Fig. A4b) to compare vertical profile of pre-linear-weighting-adjustment sum of natural ozone, domestic anthropogenic ozone and foreign anthropogenic ozone with China average total ozone from CTL.

In all of our results, the linear weighting method is applied to remove the effect of ozone nonlinearity, therefore the total ozone simulated in CTL is equal to the “adjusted” sum of natural ozone, domestic anthropogenic ozone and foreign anthropogenic ozone.

As shown in the revised Sect. 2.2 Line 206–215,

“Figure 2a shows the spatial distribution of the ratio of total surface ozone in CTL to the pre-linear-weighting-adjustment sum of natural ozone, domestic anthropogenic ozone and foreign anthropogenic ozone. The ratio is close to unity over central and western China. Over most of the eastern regions, the ratio is between 1.05 and 1.10, although it can reach 1.30 at a few locations. Figure 2b further compares the vertical profile of China average total ozone in CTL and the profile of pre-linear-weighting-adjustment sum of natural ozone, domestic anthropogenic ozone and foreign anthropogenic ozone. The difference between the two profiles is rather small. These results suggest relative small effects of chemical nonlinearity. And the linear weighting adjustment further removes these effects.”

We have revised the caption of old Fig. 11c (new Fig. 13c) as: “Of the ozone over China due to anthropogenic emissions of each foreign region, the portion produced within each foreign source region’s territory calculated based on a combination of zero-out and tagged simulations.” Please see our further explanations of the use of zero-out and tagged simulations in the response to Q1 and Q2 above.

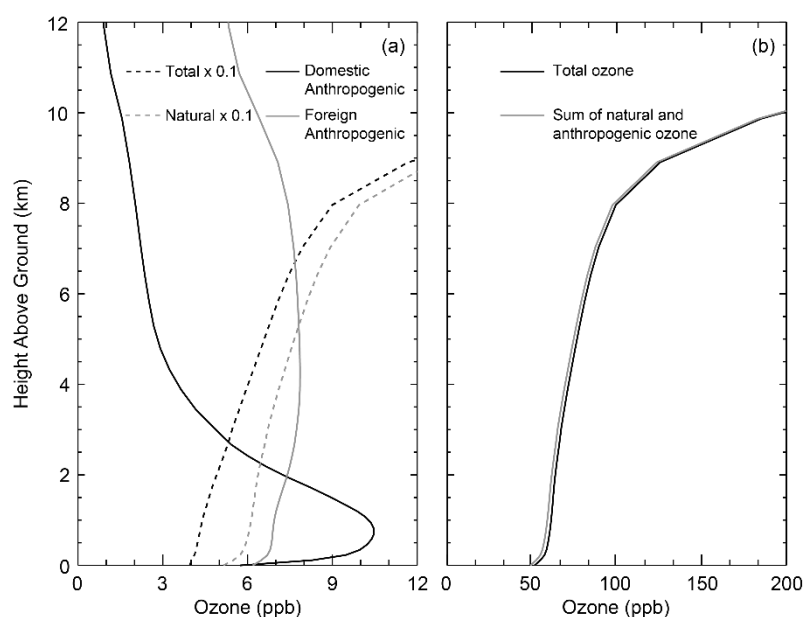


Figure A4. (a) Vertical distribution of China average daily mean ozone contributed by domestic anthropogenic emissions, foreign anthropogenic emissions, natural sources (scaled by 0.1) and total source (scaled by 0.1). (b) Vertical distribution of China

---

average daily mean total ozone simulated by control run and the sum of ozone contributed by domestic anthropogenic emissions, foreign anthropogenic emissions, natural sources which are calculated from sensitivity simulations.

**Technical Corrections:**

Throughout the manuscript there are many acronyms that are used but not defined (e.g. MOZART, NAQPMS, PKUCPL).

Modified as suggested. Thank you.

L91: The ozone itself doesn't differ, but the plumes and chemical regimes, which produce and destroy the ozone, does differ.

These sentences address the difference between 1) the transboundary ozone due to a particular region's emissions and 2) the ozone produced in the troposphere within the territory of that region from global precursor emissions.

L156-171: This paragraph mostly duplicates the information already in Table 1, and I do not feel that this redundancy is necessary.

Although we provided the emission inventories in Table 1, we felt that due to their importance to this study, it is better to also briefly describe these inventories in the main text to enhance readability and understanding.

L198-199: Figure 3 should be Figure 2

Fixed as suggested. Thank you.

L250: These numbers do not match those found in Table 3

Thanks for reminding us. We have modified the numbers both in the main text and in Fig. 3 and 4. The differences were due to a difference by mistake in the treatment of rounding.

L265-266: The authors claim that the biases are due to overestimated free tropospheric and stratospheric transport, but it's not clear to me how this conclusion was reached.

All stations shown in revised paper Line 285–287 are background stations with high altitude of more than 1500m. Ozone concentrations measured at these stations represent the background situation of the free troposphere, which is influenced by ozone transport from stratosphere.

The color scales in Figures 8a,b,d,e need to be consistent, as it requires extra effort to compare the Chinese Anthropogenic and Foreign Anthropogenic contributions. There is a risk that a casual reader would assume that the color scales in Figures 8a,b,d,e are the same, which would lead to incorrect conclusions.

Using the same color scales leads to loss of detailed information in the spatial variability of foreign anthropogenic O<sub>3</sub> and Ox, as shown in Fig. A5 below. Since this detailed information is of great interest in this study, we have elected to retain the original color scales and added a note in the caption that the color scales are different between (a, d) and (b, e).

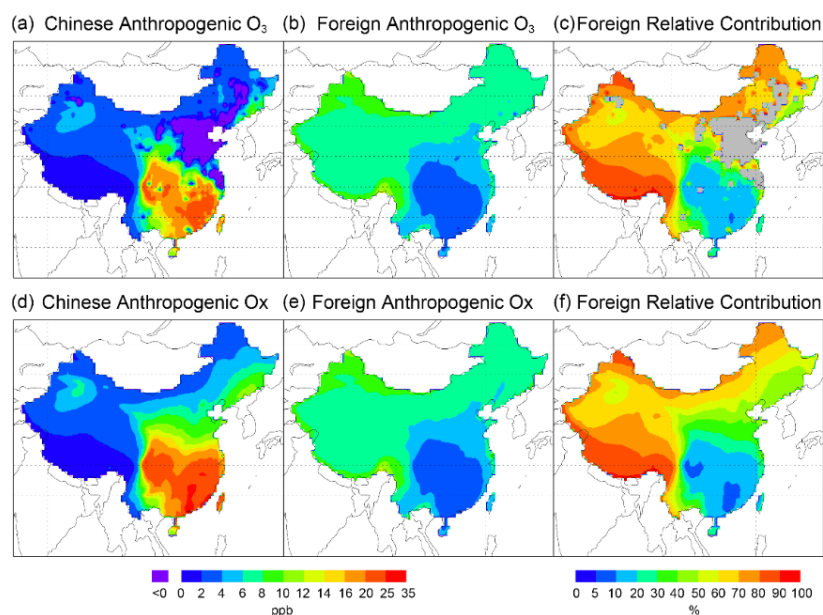


Figure A5. Spatial distribution of springtime daily mean surface ozone over China contributed by (a) domestic and (b) foreign anthropogenic emissions. (c) Percentage contribution of foreign anthropogenic emissions to total anthropogenic ozone; areas with negative Chinese contributions (due to NO<sub>x</sub> titration) are marked in grey. (d–f) similar to (a–c) but for Ox (= O<sub>3</sub> + NO<sub>2</sub>). The linear weighting adjustment is applied to derive all results.

L384: I don't feel that describing the air over the Sichuan Basin as "more isolated" is the correct description; rather the ozone chemistry of the region is controlled and dominated by domestic emissions and chemistry rather than foreign emissions.

Here we only consider surface ozone enhancement (in absolute terms, i.e., ppb) by foreign anthropogenic emissions, how much Chinese emissions contribute to ozone in this area is not relevant.

The relatively low ozone contribution from foreign emissions over Sichuan Basin compared to elsewhere may be caused by the "more isolated" terrain. Sichuan Basin is surrounded by high elevation mountains (new Fig. 3). The Qinghai-Tibet Plateau in the west and the Yunnan-Guizhou Plateau in the south block the airflows from South Asia and South-East Asia (new Fig. 10b and c). Qinling Mountains make the airflow from the north difficult to be transported to Sichuan Basin. (new Fig. 10e and f).

## Anonymous Referee #2

The manuscript presents a modeling analysis and attributes ozone in China to anthropogenic emissions outside China. Basically, it represents a breakdown of background ozone in China to different foreign regions. Although this breakdown analysis has its value, my main concerns are (1) the analysis was limited to the seasonal mean ozone attribution rather than high ozone events, (2) the modeling was based on a single, non-recent, year (2008), and (3) the nonlinearity in source attribution seems to be large and needs to be assessed more carefully. These issues need to be addressed and corrected before this work can be accepted by ACP.

We thank the reviewer for thoughtful comments, which have been incorporated in the revised manuscript.

## Major comments

1. The last sentence of the abstract, "Global emission reduction is critical for China's ozone mitigation", should be removed. The reported contribution of foreign emissions on ozone in China is essentially the background ozone. It has been well established (e.g. by several HTAP reports and references therein) that background ozone is substantial (20-50 ppbv) everywhere in the northern mid-latitude continents. For long-lived air pollutants such as ozone, essentially every country pollutes others and vice versa. To effectively mitigate ozone pollution in China, the key is to understand which source region drives the variability, especially of the high ozone days. I would be surprised if the foreign contribution is a primary factor for day-to-day changes of peak ozone over the majority of China. It appears that the paper only focuses on the seasonal mean contributions from foreign sources, thus the last sentence is a premature statement and may be interpreted misleadingly that domestic emissions control is not important.

Foreign contributed ozone can affect both the (seasonal) mean value of ozone in the receptor region as well as the peak ozone days. This study focuses on the mean impacts. Although the peak ozone days are an important aspect of ozone pollution, the mean value is of great interest. A large amount of existing ozone transport model studies are also focused on mean ozone (seasonal mean, seasonal MDA8, annual mean, etc.) (Verstraeten et al., 2016; Li et al., 2016b; Zhu et al., 2016). In fact, new epidemiological studies have suggested a strong impact of long-term mean ozone on human health, and that there is no threshold of ozone concentrations below which ozone exposure is not harmful (Bell et al., 2006; Yang et al., 2012; Peng et al., 2013; Di et al., 2017; Shindell et al., 2018).

Although a qualitative understanding has been reached that long-range transport of ozone is important, quantitative assessments are still scarce for transboundary impacts on China, as shown in the introduction section, especially compared to the large number of studies for the United States and some other countries. Although HTAP and earlier studies have worked on long-range transport impacts on Asia, the quantitative understanding for China is still poor due to this lack of China-focused studies. Also important, here we have used a comprehensive suite of near-surface and vertical profile measurements to constrain the model prior to source attribution calculations. Furthermore, as stated the introduction, we have analyzed not just the total impact of each particular foreign region but also separated the contribution of ozone produced within that source region and the contribution of ozone produced outside that source region (along the transport pathway). To our knowledge, this is the first time for China-focused transport studies.

We did not state that domestic emission control is not important. Instead, we argued, based on our detailed quantitative attribution calculations, that global emission control is important for Chinese ozone pollution mitigation. We have revised the statement to "In addition to domestic emission control, global emission reduction is critical for China's ozone mitigation".

## References:

- Bell, M. L., Peng, R. D., and Dominici, F.: The exposure-response curve for ozone and risk of mortality and the adequacy of current ozone regulations, *Environ. Health Persp.*, 114, 532–536, <https://doi.org/10.1289/ehp.8816>, 2006
- Di, Q., Wang, Y., Zanobetti, A., Wang, Y., Koutrakis, P., Choirat, C., Dominici, F., Schwartz, J. D.: Air Pollution and Mortality in the Medicare Population, *New England Journal of Medicine*, 376, 2513-2522, [10.1056/NEJMoa1702747](https://doi.org/10.1056/NEJMoa1702747), 2017

Peng, R. D., Samoli, E., Pham, L., Dominici, F., Touloumi, G., Ramsay, T., Burnett, R. T., Krewski, D., Le Tertre, A., Cohen, A., Atkinson, R. W., Anderson, H. R., Katsouyanni, K., and Samet, J. M.: Acute effects of ambient ozone on mortality in Europe and North America: results from the APHENA study, *Air Qual. Atmos. Hlth.*, 6, 445–453, <https://doi.org/10.1007/s11869-012-0180-9>, 2013.

Shindell, D., Faluvegi, G., Seltzer, K., Shindell, C.: Quantified, localized health benefits of accelerated carbon dioxide emissions reductions, *Nature Climate Change*, 8, 291–295, [10.1038/s41558-018-0108-y](https://doi.org/10.1038/s41558-018-0108-y), 2018

Yang, C. X., Yang, H. B., Guo, S., Wang, Z. S., Xu, X. H., Duan, X. L., and Kan, H. D.: Alternative ozone metrics and daily mortality in Suzhou: The China Air Pollution and Health Effects Study (CAPES), *Sci. Total Environ.*, 426, 83–89, <https://doi.org/10.1016/j.scitotenv.2012.03.036>, 2012

2. To follow up the previous comment, by reporting just seasonal mean contributions of foreign sources on ozone in China, I feel the paper does not add much new knowledge to the field, especially considering their analysis was based on a single year's simulation (see my next comment). The paper would be interesting if they had analyzed the foreign contribution to peak ozone events (during pollution episode) in addition to the mean ozone.

Please see our response regarding “peak ozone” above.

As added in our newly added Sect. 4.3 Line 482–491, here we show the domestic versus foreign contributions to modeled extreme ozone values in spring 2008 (defined as the average of the top 5% hourly ozone concentrations) (Fig. A6a–c). For comparison, we also adopt the results for mean ozone from Fig. 9 a–c (old Fig. 8a–c) and modify the color scale to make it consistent with Fig. A6a–c, as shown in Fig. A6d–f here. As expected, Chinese domestic contribution is larger for extreme ozone than for mean ozone; the negative values also disappear over North China Plain and Northeast China (comparing Fig. A6a and d). The absolute foreign contribution (in ppb) is also enhanced across China (comparing A6b and e). The percentage foreign contribution is within 10% over southern China, about 10–50% over the north, and above 70% over the west. Nevertheless, these results for extreme ozone should be interpreted with more caution, as the model cannot simulate the dates of extreme ozone very well (Fig. 4).

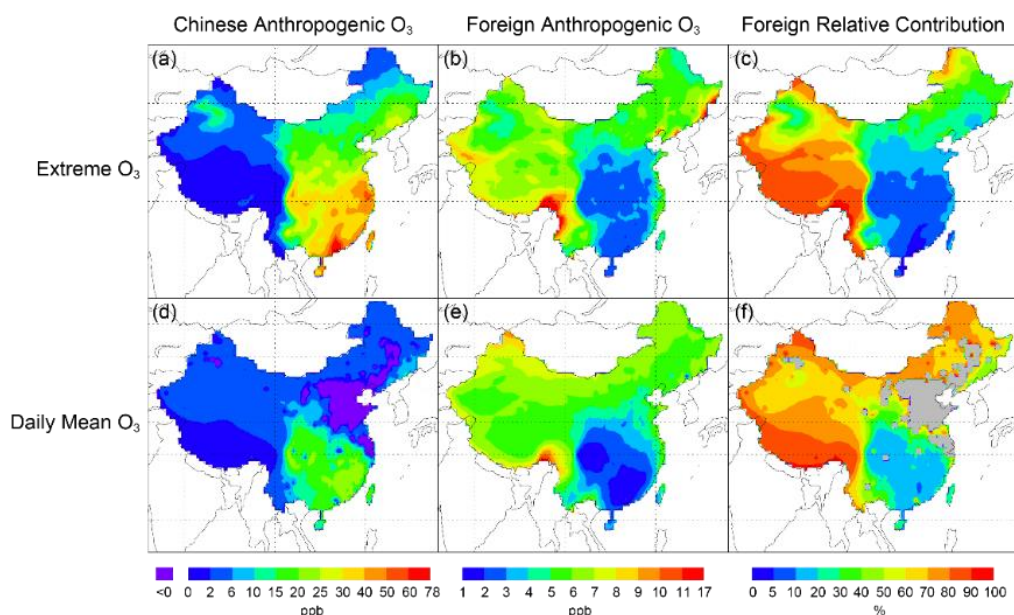


Figure A6. Spatial distribution of springtime extreme value (defined as the average of the

---

highest 5% hourly ozone concentrations) of surface ozone over China contributed by (a) domestic and (b) foreign anthropogenic emissions. (c) Percentage contribution of foreign anthropogenic emissions to total anthropogenic ozone; (d–f) similar to (a–c) but for daily mean surface ozone. Areas with negative Chinese contributions (due to NO<sub>x</sub> titration) are marked in grey. The linear weighting adjustment is applied to derive all results. Please note that the color scales are different between (a, d) and (b, e).

3. I have concerns about the choice of a single, non-recent, year (2008) used in the paper for the whole analysis. The exact magnitudes of ozone mixing ratio attributable to different sources depend on meteorology and emissions, both linked with the year of simulation. How would these ozone values change if another year is chosen to conduct the analysis? The authors stated that routine ozone measurements were scarce before 2013 (pg 6, line 203), so why not a simulation year after 2013? This would be more desirable to take advantage of more observational data for model evaluation. In particular, the increase of ozone pollution is a more recent concern in Chinese cities, after high PM events are on the decline.

We had thought about the choice of study year when conceiving the study, particularly whether to focus on a more recent year or not. At last, we decided to focus on 2008 for several reasons. First, for ozone transport model studies, it is important for model validation to have high quality observation data both near the surface and for the vertical profile that are representative of the regional ozone. The year of 2008 is when a comprehensive suite of near-surface and vertical profile measurements is available. And the observation data we used are high quality, well documented, and widely used in the literature. Although there are much more near-surface measurements from the Ministry of Environmental Protection (MEP) after 2013, there are few vertical profile measurements available in these more recent years. Also, the MEP measurements are almost all in the urban areas and cannot be used effectively to constrain the model, because our model resolution (0.5×0.667 degree) is not expected to capture the urban pollution chemistry well.

As in the newly added Sect. 4.3 (Line 492-516), previous studies have shown notable interannual variability in surface ozone over China driven by changes in precursor emissions and meteorology (Xu et al., 2008; Jin et al., 2015; Wang et al., 2017). To test how the interannual variability of meteorology and emissions would affect our source attribution findings, we have repeated all zero-out runs for spring 2012, the latest year when the GEOS-5 meteorological fields are available. Emissions for 2012 were adopted from the Community Emissions Data System (CEDS) inventory (Hoesly et al., 2018); 2012 is also the latest year the CEDS emissions for China are adjusted by the MEIC inventory. Table A1 shows the anthropogenic emissions in the two years. All zero-out simulation results in 2012 underwent the same linear weighting adjustment as for those in 2008. Figure A1d–f show the results for domestic versus foreign contributed ozone in spring 2012, as compared to the results for spring 2008 (adopted from Fig. 9a–c). In absolute terms, Chinese contributed ozone are similar between 2008 and 2012 (comparing Fig. A1a and d), reflecting the slight changes in domestic precursor emissions (Table A1). From 2008 to 2012, the absolute foreign contributed ozone increase along the southern boarder due to much enhanced emissions in South-East Asia and South Asia. The absolute foreign contributions decrease over the north and south, reflecting the net effect of changes in European and North American emissions (within 20% for both NO<sub>x</sub> and NMVOC), increased emissions in Rest of Asia, and changes in meteorology. In relative terms (Fig. A1c and f), the percentage foreign anthropogenic contributions to total anthropogenic ozone decrease from 2008 to 2012 over southern China. Nonetheless, in both years the percentage foreign contributions exceed 50% over western China and are 5–40% over southern China. Therefore our general finding that both foreign and domestic contributions to Chinese anthropogenic ozone are important holds true for these two years.

Further remarks: China is facing a severe ozone pollution problem, which has been getting worse in recent years. To tackle this problem domestic emission reductions (for both NO<sub>x</sub> and NMVOC) are of tremendous importance. Nonetheless, our results here show that foreign emission control is also necessary to ensure the success of ozone mitigation. This is particularly important during the time of fast economic growth and industrial development in nearby countries.

4. I am also concerned with the statement that over the polluted eastern China, "Chinese anthropogenic emissions lead to reductions (instead of enhancements) of surface ozone" (pg 10, line 374-375). The authors attributed this to the ozone titration effect by freshly emitted NO. The phenomena do occur in urban areas, but the GEOS-Chem simulation used in this study has a relatively coarse grid cell even for the nested-grid option (~50km x 50 km). This resolution would substantially smear out NO<sub>x</sub> emissions in a grid, leading to muted titration effect. My interpretation of that statement is that it suggests the nonlinearity in the zero-out simulations is strong (because it leads to negative ozone changes) and needs to be tested via different sensitivity runs and dealt with carefully. For example, the authors could try zeroing-out foreign anthropogenic emissions instead of Chinese anthropogenic emissions or try reducing Chinese emissions by a certain percentage rather than a complete zero-out, and then analyze if the different perturbation runs give consistent results over North China.

We agree that our model resolution cannot resolve the urban chemistry very well, which one of the reasons we had chosen not to focus our study on a more recent year and use the urban measurements from the MEP to validate the model. Nonetheless, at our model resolution, the spatial distribution of precursor emissions still show spatial contrast clearly, especially for NO<sub>x</sub> emissions, as shown in the plots below (adopted from Yan et al., 2016).

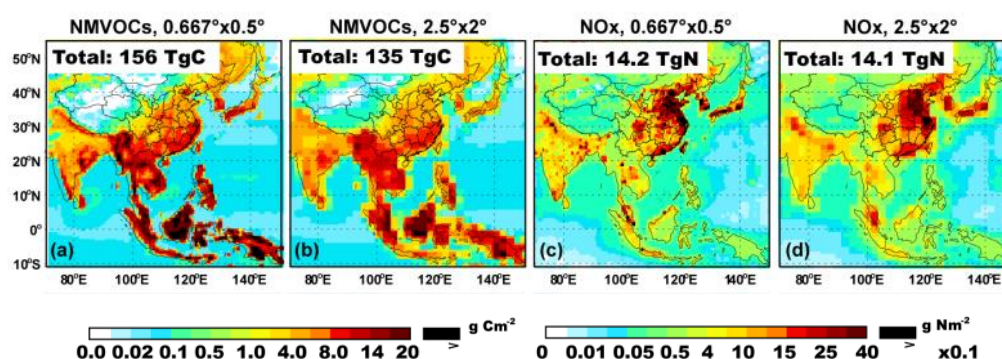


Figure A7. Total (anthropogenic and natural) emissions of NMVOCs and NO<sub>x</sub> over Asia, as represented in the nested model. Values outside the upper bound of color intervals are shown in black. Color intervals are nonlinear to better present the data range; an interval without labeling represents the mean of adjacent two intervals. Also depicted in each panel is the regional total. (Plots are adopted from Yan et al., 2016)

As suggested by the reviewer, we ran one more set of simulations by decreasing 20% anthropogenic emissions over each of the eight emission source regions (see the detailed information in Table A2). We also applied the linear weighting method to account for the non-linearity of ozone chemistry.

Figure A8a and d compares the Chinese anthropogenic contributed ozone calculated from 20%-perturbation and from zero-out simulations. Compared to the zero-out method, the 20% perturbation method leads to less Chinese contributed ozone, with negative values over more regions and smaller positive values over southern China. This result confirms our general finding that in spring 2008, the excessive domestic NO<sub>x</sub> emissions lead to relatively weak ozone production and/or strong ozone titration. Comparing to the zero-out method, the absolute foreign anthropogenic ozone obtained from 20%-perturbation

simulations are smaller by 2–3 ppb over the northern border of China (comparing Fig. A8b and e), whereas the percentage foreign contributions increase from 10–20% to 20–40% over southeastern China (comparing Fig A8c and f). Nonetheless, the spatial patterns are similar between the two methods for both the absolute and the relative foreign contributions.

We have added these results in the newly added Sect. 4.3 Line 462–481.

**Table A2.** Model simulations

Full chemistry simulation	Description
CTL	Full-chemistry simulation with all emissions
x <sub>20</sub> ANTH	Without 20% global anthropogenic emissions
x <sub>20</sub> CH	Without 20% anthropogenic emissions of China
x <sub>20</sub> JAKO	Without 20% anthropogenic emissions of Japan and Korea
x <sub>20</sub> SEA	Without 20% anthropogenic emissions of South-East Asia
x <sub>20</sub> SA	Without 20% anthropogenic emissions of South Asia
x <sub>20</sub> ROA	Without 20% anthropogenic emissions of Rest of Asia
x <sub>20</sub> EU	Without 20% anthropogenic emissions of Europe
x <sub>20</sub> NA	Without 20% anthropogenic emissions of North America
x <sub>20</sub> ROW	Without 20% anthropogenic emissions of Rest of World

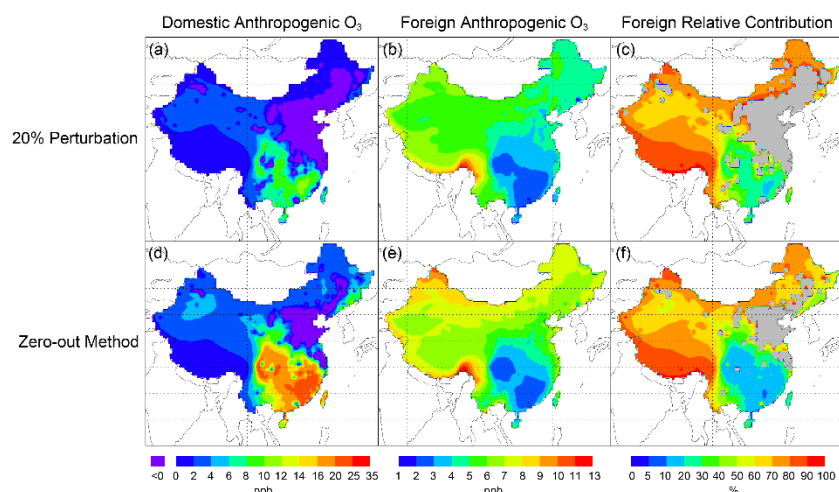


Figure A8. Spatial distribution of springtime daily mean surface ozone over China contributed by (a) domestic and (b) foreign anthropogenic emissions getting from 20%-perturbation method. (c) Percentage contribution of foreign anthropogenic emissions to total anthropogenic ozone; (d–f) similar to (a–c) but for zero-out method. Areas with negative Chinese contributions (due to NO<sub>x</sub> titration) are marked in grey. The linear weighting adjustment is applied to derive all results. Please note that the color scales are different between (a, d) and (b, e).

### Minor Issues

Pg 5, line 190-195: The description of the weighting method to account for nonlinear chemistry is very vague, and I don't understand the scientific basis for this method. It should be expanded and explained in a way such that it is understandable to readers who have not read the original Li et al (2016) paper.

Ozone production is nonlinearly dependent on its precursors. Thus, the sum of natural ozone and anthropogenic ozone due to each emission source region calculated from zero-out simulations is not equal to ozone concentration calculated in the control run (CTL). Considering uncertainties induced by emission perturbation methods, we used a linear weighting method to adjust ozone concentration attributed to different sources, making the sum of natural ozone and anthropogenic ozone equal to amount of ozone simulated in CTL.

As clarified in the revised manuscript, here is an example to adjust Chinese contribution to ozone over China using the linear weighting approach. Equation A1 calculates the fractional Chinese contribution ( $\alpha$ ) to the sum of ozone from individual anthropogenic source regions and from natural sources; the simulations involved are all full-chemistry runs (CTL, xCH, xEU, ..., xANTH). Equation A2 applies the fractional contribution  $\alpha$  to the total ozone in CTL to obtain the final adjusted Chinese contribution. These equations are used in the revised manuscript for better clarity; they are simply a transformed version of Eq. 1 in the original manuscript.

Similar adjustments were applied to other source regions, such that all results shown in our original manuscript are for “adjusted” ozone attribution through this linear weighting approach.

As shown in our revised manuscript Line 216–218, “A similar approach was used by Li et al. (2016a) to estimate the contribution of China to global radiative forcing, although in their study 20% (instead of 100%) of emissions over individual emission source regions are removed in the sensitivity simulations.”

$$\alpha = \frac{\text{Con(CTL)} - \text{Con(xCH)}}{\sum_{i=1}^8 [\text{Con(CTL)} - \text{Con(Ci)}] + \text{Con(xANTH)}} \quad (\text{A1})$$

$$C_{\text{CH}} = \alpha \times \text{Con(CTL)} = \frac{\text{Con(CTL)} - \text{Con(xCH)}}{\sum_{i=1}^8 [\text{Con(CTL)} - \text{Con(Ci)}] + \text{Con(xANTH)}} \times \text{Con(CTL)} \quad (\text{A2})$$

Pg 3, line 108-109: this sentence is confusing. Do you mean there are 10 producing regions and 8 source regions? Why and how are they different?

The eight source regions represent emitter of precursor gases. The 10 producing regions include the troposphere of eight emitters, the troposphere of total oceanic regions, and the stratosphere. We have clarified these terms in the revised manuscript.

Language Issues: The paper has a few grammar errors and language issues, some examples listed below. I would suggest the authors proofread it more carefully during the revision stage.

We have checked grammar errors and language issues of the paper again and fixed them in the revised version. Thanks for reminding.

Pg 1, line 6: "mean bias at 10-15%" should be "mean bias of 10-15%"

Fixed as suggested. Thank you.

Pg 2, line 38: "at surface" should be "at the surface".

Fixed as suggested. Thank you.

---

Pg 10, line 356: "nature ozone" should be "natural ozone".

Fixed as suggested. Thank you.

# Foreign and domestic contributions to springtime ozone over China

Ruijing Ni<sup>1</sup>, Jintai Lin<sup>1</sup>, Yingying Yan<sup>1</sup>, Weili Lin<sup>2</sup>

<sup>1</sup>Laboratory for Climate and Ocean-Atmosphere Studies, Department of Atmospheric and Oceanic Sciences, School of Physics, Peking University, Beijing 100871, China

<sup>2</sup>College of Life and Environmental Sciences, Minzu University of China, Beijing 100081, China

Correspondence to: J.-T. Lin ([linjt@pku.edu.cn](mailto:linjt@pku.edu.cn))

**Abstract.** China is facing a severe ozone problem, but the origin of its ozone remains unclear. Here we use a GEOS-Chem based global-regional two-way coupled model system to quantify the individual contributions of eight emission source regions worldwide to springtime ozone in 2008 over China. The model reproduces the observed ozone from 31 ground sites and various aircraft and ozonesonde measurements in China and nearby countries, with a mean bias of at 10–15% both near the surface and in the troposphere. We then combine zero-out simulations, tagged ozone simulations, and a linear weighting approach to accounting for the effect of nonlinear chemistry on ozone source attribution. We find considerable contributions of total foreign anthropogenic emissions to surface ozone over China (2–11 ppb). For ozone averaged over China of anthropogenic origin, foreign regions together contribute 40–50% below the height of 2 km and 85% in the upper troposphere. For total foreign anthropogenic emissions contributed ozone over China at various heights, the portion of transboundary ozone produced within foreign emission source regions is less than 50%, with the rest produced by precursors transported out of those source regions. Japan and Korea contribute 0.6–2.1 ppb of surface ozone over the east coastal regions. South-East Asia contributes 1–5 ppb over much of southern China and South Asia contributes up to 5–10 ppb of surface ozone over border of southwestern China; and their contributions increase with height due to strong upwelling over the source regions. European contribution reaches 2.1–3.0 ppb for surface ozone over the northern border of China and 1.5 ppb in the lower troposphere averaged over China. North America contributes 0.9–2.7 ppb of surface ozone over most of China (1.5–2.1 ppb over the North China Plain), with a China average at 1.5–2.5 ppb at different heights below 8 km, due to its large anthropogenic emissions and the transport-favorable mid-latitude westerly. In addition to domestic emission control, Global emission reduction is critical for China's ozone mitigation.

## 37 1. Introduction

38 Ozone is an important atmospheric oxidant and the primary source of the hydroxyl  
39 radical (OH). At the surface, ozone also damages human health and reduces crop yield.  
40 China is currently facing a severe ozone pollution problem, with measured maximum  
41 hourly ozone exceeding 200 ppb in many cities (Wang et al., 2006; Xue et al., 2014).  
42 Even in the remote areas of western China, measured daily mean concentrations of  
43 ozone exceed 50 ppb frequently (Xue et al., 2011; Lin et al., 2015). Xu et al. (2016)  
44 showed that daytime ozone at Waliguan, a global background station, grew  
45 significantly from 1994 to 2013 at a rate of  $0.24 \pm 0.16$  ppb year<sup>-1</sup>. The severe ozone  
46 problem is largely associated with growth in anthropogenic emissions of nitrogen  
47 oxides (NO<sub>x</sub>) and non-methane volatile organic compounds (NMVOC). Chinese  
48 anthropogenic NO<sub>x</sub> emissions increased at a rate of 7.9% year<sup>-1</sup> from 2000 to 2010  
49 (Zhao et al., 2013); and its anthropogenic NMVOC emissions increased from 22.45 Tg  
50 in 2008 to 29.85 Tg in 2012 (Wu et al., 2016).

51 Ozone has a lifetime of several days to weeks in the troposphere (Young et al.,  
52 2013; Yan et al., 2016), which makes its long-distance transport across regions and even  
53 continents possible. Many observational and modeling studies have showed substantial  
54 trans-Pacific and trans-Atlantic transport of ozone and precursors (Jacob et al., 1999;  
55 Derwent et al., 2004; Lin et al., 2008; Cooper et al., 2010; Verstraeten et al., 2016). The  
56 trans-Pacific transport of East Asian air pollutants enhances springtime surface ozone  
57 concentrations over the western United States by 1–5 ppb (Zhang et al., 2008; Brown-  
58 Steiner and Hess, 2011; Lin et al., 2012b; Lin et al., 2014). Auvray and Bey (2005)  
59 reported that North American and Asian ozone account for 10.9% and 7.7% of ozone  
60 over Europe, respectively. The Hemispheric Transport of Air Pollution (HTAP) project  
61 studied the trans-continental pollution, by model sensitivity simulations applying a 20%  
62 perturbation in anthropogenic emissions in four regions (North America, Europe, South  
63 Asia, and East Asia, each defined as a broad rectangle-shaped area) (HTAP, 2010).  
64 HTAP showed that the annual average impact of North American emissions on East  
65 Asian surface ozone is comparable to the impact of East Asian emissions on North  
66 America (0.22 ppb averaged over each rectangular region).

67 Several studies investigated the influence of transboundary transport on surface ozone  
68 over Chinese territory (Wang et al., 2011; Li et al., 2014; Li et al., 2016b; Zhu et al.,  
69 2016; Yin et al., 2017). Wang et al. (2011) used tagged ozone simulations with GEOS-  
70 Chem to study the global production of surface ozone over China for 2006. They  
71 showed that in spring 2006, tropospheric ozone produced over India contributed up to  
72 6 ppb to surface ozone over western China; and that ozone produced over Europe and  
73 North America each contributed 2–5 ppb of ozone over northeastern China and North  
74 China. Using an emission zero-out method with MOZART simulations (i.e., without  
75 versus with emissions), Li et al. (2014) reported that modeled trans-Eurasian ozone

76 transport enhanced surface ozone over northwestern China by 2–6 ppb in spring 2000.  
77 Using tagged ozone simulations with MOZART, Zhu et al. (2016) revealed significant  
78 springtime ozone transport (~ 6 ppb) from Europe and Africa to Waliguan averaged  
79 from 1997 to 2007 and 3–5 ppb ozone from North and South America together. Using  
80 a tagged ozone method based on [the Nested Air Quality Prediction Modeling System](#)  
81 [\(NAQPMS\)](#), Li et al. (2016) found 0.5–3.0 ppb of ozone over northeastern China  
82 produced over the Korean peninsula in 2010. Based on observational and back-  
83 trajectory analyses, Yin et al. (2016) found that ozone at the Nam Co site over Tibet in  
84 spring is greatly affected by anthropogenic contributions from South Asia.

85 Transboundary ozone due to precursor emissions of a source region can be produced  
86 both within and outside the source region. The two mechanisms contribute roughly  
87 equally for the case of trans-Pacific ozone from East Asia to the western United States  
88 (Zhang et al., 2008; Jiang et al., 2016). And the ozone production along the transport  
89 pathway is largely associated with thermal dissociation of peroxyacetyl nitrate (PAN)  
90 that has been formed in the boundary layer of the NO<sub>x</sub> emission source region. The  
91 transport of ozone precursors means that ozone produced within a region (from emitted  
92 and transported precursors worldwide) differs from ozone produced from that region's  
93 emissions. This difference affects how ozone over a receptor region is attributed to other  
94 regions (Wang et al., 2011; Li et al., 2014). It is thus important that the contribution of  
95 ozone produced at a “producing region” from emissions of a source region be quantified  
96 explicitly.

97 Here we simulate the contributions of anthropogenic emissions in individual regions  
98 across the globe to ozone at various heights over China. As typically assumed,  
99 anthropogenic contributions are associated with anthropogenic NO<sub>x</sub>, carbon monoxide  
100 (CO) and NMVOC emissions, excluding the effect of methane. We use a GEOS-Chem  
101 based two-way coupled modeling system (Yan et al., 2014; 2016) that integrates an  
102 Asian nested model and a global model in a sense of two-way exchange, which better  
103 simulates multi-scale interactions between the nested and global domains. Our study is  
104 focused on spring 2008, in which season a comprehensive set of ground, aircraft and  
105 ozonesonde measurements over China is available for model evaluation. Also,  
106 transboundary transport of ozone is most significant in spring due to active cyclonic  
107 activities and strong westerly winds (Liang et al., 2004; Wang et al., 2011; HATP,  
108 2010).

109 We explicitly identify ozone produced in 10 individual regions of the world from  
110 anthropogenic precursor emissions in each of eight source regions. [These 10 producing](#)  
111 [regions include the troposphere of the eight emitters, the troposphere of total oceanic](#)  
112 [regions, and the stratosphere.](#) For this purpose, we combine the emission zero-out  
113 method and the tagged ozone approach (Wang et al., 1998). The zero-out or similar  
114 emission perturbation methods are widely used to quantify the contribution of  
115 emissions in a source region to a receptor region as a combined result of the two  
116 production-transport mechanisms aforementioned (Lin et al., 2008; HTAP, 2010; Lin

117 et al 2012a; Li et al., 2014). The tagged ozone approach quantifies the ozone produced  
118 in any designated region with no information about whether the associated precursors  
119 are emitted in that region or are transported from somewhere else (Wang et al., 1998;  
120 Wang et al., 2011; Li et al., 2016b). To account for ozone production nonlinearity, we  
121 use a simple linear weighting method to adjusting simulation results, similar to Li et al.  
122 (2016a).

123 The rest of our paper is organized as follows. Section 2 presents model simulations,  
124 measurement data, and the ozone source attribution method. Section 3 evaluates the  
125 modeled ozone and CO using ground, aircraft and ozonesonde observations. Section 4  
126 analyzes the modeled contributions to near-surface ozone over China by natural sources  
127 as well as anthropogenic emissions in individual regions. Section 5 shows the ozone  
128 source attribution at different heights of the troposphere. For each emission source  
129 region, it also separates the contribution of ozone produced within that source region  
130 from the contribution produced outside of that source region. Section 6 concludes the  
131 study.

## 132 **2. Model simulations, measurements, and source attribution method**

### 133 *2.1 Two-way coupled GEOS-Chem modeling system*

134 The two-way coupled system (Yan et al., 2014; Yan et al., 2016) is built upon version  
135 9-02 of GEOS-Chem ([http://wiki.seas.harvard.edu/geos-chem/index.php/Main\\_Page](http://wiki.seas.harvard.edu/geos-chem/index.php/Main_Page)).  
136 Here we couple the global GEOS-Chem model (~~at 2.5° long. × 2° lat.~~~~at 2.5° long. ×~~  
137 ~~2° lat.~~) with its nested model covering Asia (70°E–150°E, 11°S–55°N, ~~0.667° long.~~  
138 ~~× 0.5° lat.~~~~at 0.667° long. × 0.5° lat.~~). Through the [PeKing University CouPLer](#)  
139 [\(PKUCPL\)](#) for two-way coupling, for every three hours the global model provides  
140 lateral boundary conditions for the nested model, while the nested model results  
141 replace the global model results within the nested domain (Yan et al., 2014; 2016).  
142 Both models are driven by the GEOS-5 assimilated meteorological fields at respective  
143 horizontal resolutions from National Aeronautics and Space Administration Global  
144 Modeling and Assimilation Office. There are 47 vertical layers for both models, and  
145 the lowest 10 layers are about 130 m thick each.  
146 Both the global and nested GEOS-Chem models include the full gaseous HO<sub>x</sub>-O<sub>x</sub>-  
147 NO<sub>x</sub>-CO-NMVOC chemistry (Mao et al., 2013) and online aerosol calculations, with  
148 further updates detailed in Lin et al. (2012) and Yan et al. (2016). As aromatics are not  
149 explicitly represented in the model, following Lin et al. (2012), we approximate the  
150 ozone production of aromatics by increasing anthropogenic emissions of propene by a  
151 factor of four, based on their reactivity differences, their similarity in emission spatial  
152 variability, and recently estimated emission amounts of aromatics (Liu et al., 2010). We  
153 use the Linoz scheme for ozone production in the stratosphere (McLinden et al., 2000).  
154 We adjust the stratospheric production rate in the nested model to ensure that the  
155 stratosphere-troposphere exchange (STE) of ozone in the nested model matches the  
156 STE in the global model over the same nested domain (Yan et al., 2016). Vertical

157 mixing in the planetary boundary layer (PBL) is parameterized by a non-local scheme  
158 (Holtlag and Boville, 1993; Lin and McElroy, 2010), and convection in the model  
159 employs the relaxed Arakawa-Schubert scheme (Moorthi and Suarez, 1992).

160 Table 1 lists the emission inventories used here. Global anthropogenic emissions of  
161 NO<sub>x</sub> and CO in 2008 are from the Emission Database for Global Atmospheric Research  
162 (EDGAR v4.2). Anthropogenic NMVOC emissions are from the REanalysis of  
163 Tropospheric chemical composition (RETRO) inventory for 2000. Anthropogenic  
164 emissions over China, the rest of Asia, the United States, Canada, Mexico and Europe  
165 are replaced by regional inventories MEIC (for 2008), INTEX-B (for 2006), NEI2005  
166 (for 2005), CAC (for 2008), BRAVO (for 1999) and EMEP (for 2007), respectively.  
167 Emissions of CO and NO<sub>x</sub> are scaled to 2008 in the United States and to 2006 in Mexico.  
168 ([http://wiki.seas.harvard.edu/geos-](http://wiki.seas.harvard.edu/geos-chem/index.php/Scale_factors_for_anthropogenic_emissions)  
169 [chem/index.php/Scale factors for anthropogenic emissions](http://wiki.seas.harvard.edu/geos-chem/index.php/Scale_factors_for_anthropogenic_emissions)). We use daily biomass  
170 burning emissions from Global Fire Emission Database version 3 (GFED3) (van der  
171 Werf et al., 2010). Biogenic emissions of NMVOC are calculated online based on the  
172 MEGAN v2.1 scheme (Guenther et al., 2012). For lightning NO<sub>x</sub> emissions, flash rates  
173 are calculated based on the cloud top height and constrained by climatological satellite  
174 observations (Murray et al., 2012), and the vertical profile of emitted NO<sub>x</sub> follows Otto  
175 et al. (2010). Online calculation of soil NO<sub>x</sub> emissions follows Hudman et al. (2012).

## 176 2.2 Zero-out simulations, tagged ozone simulations, and weighted adjustment

177 Table 2 presents 10 full-chemistry simulations to quantify Chinese and foreign  
178 anthropogenic contributions to springtime ozone over China in 2008. A base simulation  
179 (CTL) includes all emissions. The second simulation excludes anthropogenic NO<sub>x</sub>, CO  
180 and NMVOC emissions worldwide to determine the natural ozone (xANTH). Eight  
181 additional simulations exclude anthropogenic emissions over China (xCH), Japan and  
182 Korea (xJAKO), South-East Asia (xSEA), South Asia (xSA), Rest of Asia (xROA),  
183 Europe (xEU), North America (xNA) and Rest of World (xROW), respectively (see  
184 regional definitions in Fig. 1). All simulations cover November 2007 through May 2008,  
185 with the first four months used for spin-up, except for additional CTL simulations in  
186 other years for model evaluation purposes.

187 Table 2 also shows 10 tagged simulations (denoted as T\_CTL, T\_xANTH, etc.) with  
188 respect to CTL and other eight zero-out sensitivity simulations. Each tagged simulation  
189 includes 10 tracers to track ozone produced within the troposphere of eight source  
190 regions, produced within the troposphere of the oceanic regions, or transported from  
191 the stratosphere. Considering the time for STE of air, all tagged ozone simulations are  
192 spun up for 10 years.

193 Ozone production is nonlinearly dependent on its precursors, adding uncertainties to  
194 the source attribution calculated by emission perturbation methods (Wu et al., 2009).  
195 To account for this issue, we use a linear weighting method to adjust all ozone  
196 attribution results (Li et al., 2016a), unless stated otherwise. Equation 1 Below is an

197 example to determine the contribution from Chinese anthropogenic emissions (here  $C_i$   
 198 represents the sensitivity simulation for one of the eight emission source regions). The  
 199 adjustment is done for each grid cell over China. Equation 1 calculates the fractional  
 200 Chinese contribution ( $\alpha$ ) to the sum of ozone from individual anthropogenic source  
 201 regions and from natural sources; the simulations involved are all full-chemistry runs  
 202 (CTL, xCH, xEU, ..., xANTH). Equation 2 applies the fractional contribution  $\alpha$  to the  
 203 total ozone in CTL to obtain the final adjusted Chinese contribution.

$$204 \quad \alpha = \frac{\text{Con(CTL)} - \text{Con(xCH)}}{\sum_{i=1}^8 [\text{Con(CTL)} - \text{Con}(C_i)] + \text{Con(xANTH)}} \quad (1)$$

$$205 \quad C_{\text{CH}} = \alpha \times \text{Con(CTL)}$$

$$206 \quad = \frac{\text{Con(CTL)} - \text{Con(xCH)}}{\sum_{i=1}^8 [\text{Con(CTL)} - \text{Con}(C_i)] + \text{Con(xANTH)}} \times \text{Con(CTL)} \quad (2)$$

207 Figure 2a shows the spatial distribution of the ratio of total surface ozone in CTL to  
 208 the pre-linear-weighting-adjustment sum of natural ozone, domestic anthropogenic  
 209 ozone and foreign anthropogenic ozone. The ratio is close to unity over central and  
 210 western China. Over most of the eastern regions, the ratio is between 1.05 and 1.10,  
 211 although it can reach 1.30 at a few locations. Figure 2b further compares the vertical  
 212 profile of China average total ozone in CTL and the profile of pre-linear-weighting-  
 213 adjustment sum of natural ozone, domestic anthropogenic ozone and foreign  
 214 anthropogenic ozone. The difference between the two profiles is rather small. These  
 215 results suggest relative small effects of chemical nonlinearity. And the linear weighting  
 216 adjustment further removes these effects.

217 A similar approach was used by Li et al. (2016a) to estimate the contribution of China  
 218 to global radiative forcing, although in their study 20% (instead of 100%) of emissions  
 219 over individual emission source regions are removed in the sensitivity simulations.

$$220 \quad C_{\text{CH}} = \frac{\text{Con(CTL)}}{\sum_{i=1}^8 [\text{Con(CTL)} - \text{Con}(C_i)] + \text{Con(xANTH)}} \times [\text{Con(CTL)} - \text{Con(xCH)}] \quad (1)$$

## 221 2.3 Measurements

222 This study presents model evaluation over China and its neighboring countries in spring.  
 223 We also evaluate the simulation of CO, a relatively long-lived transport tracer. Figure  
 224 32-3 shows the suite of ground, aircraft and ozonesonde measurements.

### 225 2.3.1 Surface measurements

226 Measurements from a total of 32 ground sites are used here; see Tables 3 and 4 for  
 227 geographical information. Routine observations of ozone and CO in China were  
 228 scarcely available before 2013. Hourly data are available for this study from five  
 229 rural/background sites across China maintained by the Chinese Meteorological  
 230 Administration (Xu et al., 2008; Lin et al., 2009; Fang et al., 2014; Ma et al., 2014).  
 231 These sites include a rural site (Gucheng over North China Plain), three regional

232 background sites (Longfengshan over the northeast, Lin'an over the east, and Shangri-  
233 La over the southwest), and a Global Atmosphere Watch (GAW) background site  
234 (Waliguan over the west). Data are available for 2007 at Gucheng and Longfengshan  
235 and for 2008 at other three sites.

236 We also use hourly ozone and CO measurements in spring 2008 from six GAW  
237 background sites in the vicinity of China from the World Data Center for Greenhouse  
238 Gases (WDCGG, <http://ds.data.jma.go.jp/gmd/wdcgg/cgi-bin/wdcgg/catalogue.cgi>).  
239 These sites include Issyk-Kul in Kyrgyzstan, Everest-Pyramid in Nepal, Bukit Koto  
240 Tabang in Indonesia, and Yonagunijima, Tsukuba and Ryori in Japan.

241 To obtain a more comprehensive observation dataset for model evaluation, we further  
242 use monthly mean ozone data in spring 2008 from 15 remote/rural sites from the Acid  
243 Deposition Monitoring Network in East Asia (EANET,  
244 <http://www.eanet.asia/product/index.html>). We also collect monthly ozone observation  
245 data at six sites over China from the literature, including data at three mountain sites  
246 (Mts. Tai, Hua, and Huang).

### 247 *2.3.2 Measurements of vertical profiles*

248 To evaluate vertical distribution of ozone and CO over China, we use observations from  
249 the Measurements of Ozone and Water Vapor by Airbus In-Service Aircraft (MOZAIC)  
250 program (Marenco et al., 1998). Data during both ascending and descending processes  
251 of the aircrafts are available during spring 2000–2005 at three airports (Beijing,  
252 Shanghai, and Hong Kong). The vertical resolution is 150 m.

253 We further use the ozonesonde data at six sites in spring 2008 from the World Ozone  
254 and Ultraviolet Data Center (WOUDC,  
255 <http://www.woudc.org/data/explore.php?lang=en>) operated by the Meteorological  
256 Service of Canada. The six sites include Hanoi in Vietnam, Hong Kong in China,  
257 Sepang Airport in Malaysia, and Sapporo, NAHA and Tateno in Japan. Ozonesondes  
258 are launched every few days, thus the data are relatively scarce. We also use the GPSO3  
259 ozonesonde data in spring 2008 over Beijing measured by the Institute of Atmospheric  
260 Physics (IAP) of the Chinese Academy of Sciences (Wang et al., 2012). All ozonesonde  
261 measurements were launched at around 14:00 local time.

## 262 **3. Model evaluation**

263 Here we focus on model evaluation over China and its neighboring area in spring.  
264 Global ozone evaluation of the two-way coupled model system is detailed in Yan et al.  
265 (2016) using 1420 ground sites, various aircraft observations and satellite  
266 measurements, although the observations over China are sparse.—

### 267 3.1 Surface ozone and CO over China and nearby countries

268 Figure 3-4 compares the springtime time series of modeled (solid red line) and observed  
269 (solid black line) maximum daily average 8-hour (MDA8) ozone concentrations at 10  
270 sites with daily measurements. Model data are sampled at times and locations  
271 coincident with valid observations.

272 Figure 3a4a–b evaluates the model results at Gucheng and Longfengshan. To compare  
273 to observations in spring 2007 at these two sites, we conduct an additional full  
274 chemistry simulation for 2007. At these sites, the model captures the observed MDA8  
275 ozone, with a normalized mean bias (NMB) of 23% at Gucheng and 45% at  
276 Longfengshan. The respective correlation coefficients (R) for day-to-day variability are  
277 0.51 and 0.59; the modest correlation is primarily because the model does not capture  
278 a few short-term spikes.

279 At Lin'an (Fig. 3e4c), the modeled spring average MDA8 ozone matches the observed  
280 value (68.9 ppb versus 65.1 ppb,  $R = 0.64$ ). The model cannot reproduce the observed  
281 extreme low values on several days. This deficiency is likely due to representative  
282 errors of model meteorology. Located in a hilly area, this site often receives rains and  
283 fogs in spring, which is not captured by the model meteorology at a resolution of  $0.667^\circ$   
284 long.  $\times 0.5^\circ$  lat. We find that the extremely low observed ozone values normally occur  
285 on days with high relative humidity (black dashed line, reflecting rainy or foggy days),  
286 when the model underestimates RH (red dashed line) and overestimates ozone.

287 At Shangri-La, Waliguan and Issyk-Kul (Fig. 3d4d–f), with high ~~latitudes~~ altitudes  
288 (1640–3816 m) and little local anthropogenic sources, the model overestimates the  
289 MDA8 ozone by 7–8 ppb (11–14%). At Everest-Pyramid in Nepal (Fig. 3e4g, at  
290 5079 m altitude), the overestimate reaches 13 ppb (19%). These positive biases are due  
291 to overestimated transport from the free troposphere and stratosphere. The model  
292 captures the temporal variability of MDA8 ozone quite well ( $R = 0.72$ – $0.78$ ) at the three  
293 Japanese sites (Yonagunijima, Tsukuba and Ryori, Fig. 3h4h–j). Its NMB is within 23%  
294 at Yonagunijima and Ryori. There is an overestimate at Tsukuba (NMB = 1819%),  
295 mostly reflecting the large positive biases on a few days.

296 Table 4 shows model comparisons with monthly mean EANET ozone data. These data  
297 represent daily mean rather than MDA8 values, based on the availability of  
298 observations. At seven sites, the model results exceed the observations with a mean  
299 difference by 7 ppb (16%). At the other eight sites, the model results are smaller than  
300 the observations with a mean difference by 7 ppb (11%). These differences reflect  
301 model biases as well as a sampling bias due to lack of knowledge on which days contain  
302 valid observations.

303 Table 4 further compares the modeled monthly mean daily mean ozone in spring 2008  
304 to the observations in various years collected from the literature. Again, the comparison  
305 is affected by a sampling bias. Although not our primary focus, this extended

306 [comparison gives a sense of how model ozone is situated in the general ozone pollution](#)  
307 [phenomena in China.](#) The model reproduces the average magnitude of ozone at the  
308 three mountainous sites (Mts. Tai, Hua and Huang) with a mean bias below 5 ppb (9%).  
309 The model has a large overestimate by 48% at the [Hok Tsui coastal](#) rural site in Hong  
310 Kong ([36.0 versus 53.4 ppb](#)), although [the](#) times are different (2008 versus 1994–2007).  
311 [Wang et al. \(2009\) shows that the springtime ozone concentration at this site increased](#)  
312 [from 1994 to 2007 at a rate of 0.41 ppb/yr, partly explaining this difference. The](#)  
313 [remaining difference may reflect that the model resolution is not able to represent the](#)  
314 [complex local terrain and land-sea contrast at this site.](#) The model overestimates ozone  
315 at an urban site in Nanjing by 16%, although the observations were made in 2000–2002  
316 when Chinese anthropogenic emissions of NO<sub>x</sub> were only about half of those in 2008  
317 (Xia et al., 2016).

318 We also evaluate the modeled daily average CO at six sites within and outside China  
319 with available hourly observations (Fig. [45](#)). Overall, the model captures the day-to-  
320 day variability of daily mean CO fairly well ( $R = 0.40$  at Lin'an, 0.60 at Shangri-La,  
321 0.56 at Ryori, and 0.73–0.82 at other three sites). It has a small mean bias (within [34%](#))  
322 at Bukit Koto Tabang and Ryori, although with negative biases (by 13–33%) at other  
323 four sites. Such an underestimate is typical in global simulations (Young et al., 2013),  
324 and it may be related to excessive OH (Young et al., 2013; Yan et al., 2014; 2016)  
325 and/or underestimated emissions (Kopacz et al., 2010; Wang et al., 2011). As compared  
326 to the coarse-resolution global model alone, our two-way coupling results in less CO  
327 underestimate (Yan et al., 2014), although it does not eliminate the bias.

### 328 *3.2 Vertical profiles of ozone and CO*

329 Figure [5a6a–c](#) compares modeled ozone in 2008 to MOZAIC data over 2000–2005 at  
330 the airports of Beijing, Shanghai and Hong Kong. Although model and MOZAIC data  
331 are in different years, to achieve best sampling consistency, we sample the model results  
332 at times of day when the commercial aircrafts take off or land in with available  
333 MOZAIC data. The timing information is shown in Fig. [56](#). GEOS-Chem reproduces  
334 the vertical gradient of MOZAIC ozone in general. The model underestimates  
335 MOZAIC ozone in the PBL over Beijing Airport mainly due to inconsistent temporal  
336 sampling, as further comparison with GPSO3 ozonesonde data (Bian et al., 2007; Wang  
337 et al., 2012), where model results are sampled at times coincident with the observations,  
338 shows little model bias (within 4%, Fig. [5g6g](#)). Over Hong Kong, the model captures  
339 the weak vertical gradient between 2 km and 11 km, although it has a positive bias  
340 below 2 km due to its inability to capture the complex terrains and local pollution source  
341 characteristics around the airport. The model overestimates ozone in the middle and  
342 upper troposphere over Shanghai, with larger biases at higher altitudes, likely indicating  
343 too strong STE. Other causes may include differences in meteorology and [growth in](#)  
344 [emissions between 2000–2005 and 2008, as discussed for the surface ozone in Sect. 3.1.](#)

345 Figure [6–7](#) compares the modeled ozone profiles to WOUDC data at six sites. Here

346 model results are sampled at ozonesonde launch times, and ozonesonde data are  
347 regridded to match the model vertical resolution. Overall, GEOS-Chem captures the  
348 vertical gradient of ozone fairly well. The model reproduces the overall weak vertical  
349 gradients at Hanoi, Hong Kong, Sepang and NAHA. It also reproduces the rapid  
350 increases above 8 km at Sapporo and Tateno, although it has positive biases at 10–20  
351 ppb. GEOS-Chem reproduces the observed middle and upper tropospheric ozone at  
352 Hong Kong and Sepang, although it has an overestimate in the lower troposphere,  
353 consistent with the bias shown in Fig. 5e6c.

354 Figure 5d6d–f also compares the modeled CO with the MOZAIC data. Similar to the  
355 evaluation results for surface CO, GEOS-Chem generally underestimates the MOZAIC  
356 CO at most heights above the three airports, although it captures the vertical shape fairly  
357 well.

### 358 3.3 Summarizing remark on model evaluation

359 Our simulation has a small NMB for surface ozone, at about 10% averaged over 10  
360 sites with hourly data (Fig. 43 and Table 3) and about 15% averaged over 21 sites with  
361 monthly data from EANET and the literature (Table 4). The model also captures the  
362 general vertical distribution of ozone at ten places over China and nearby regions, with  
363 a tropospheric mean bias at 12%. These agreements allow using the model for source  
364 attribution studies in the next sections. On the other hand, with a horizontal resolution  
365 of about 50 km over Asia, the model often fails to simulate the complex terrains, local  
366 meteorological conditions, and/or local emission characteristics at several hilly or  
367 airport sites. The model also tends to overestimate the STE influences over Asia.  
368 Addressing these issues warrant future research with improved model resolutions and  
369 STE representation.

370 GEOS-Chem tends to underestimate CO over Asia (by 20% on average), similar to  
371 many other models (Kopacz et al., 2010; Young et al., 2013). We conduct a sensitivity  
372 simulation by doubling Chinese anthropogenic CO emissions, which result in a slight  
373 increase in surface ozone by 0.1–0.4 ppb and 2–3 ppb over clean and polluted areas of  
374 China, respectively. The low sensitivity of ozone to CO emissions was also found  
375 by Jiang et al. (2015). We thus conclude that our ozone simulations over China are  
376 influenced insignificantly by the underestimate in CO.

## 377 4. Source attribution modeling for surface ozone over China

### 378 4.1 Total, background and natural ozone

379 Figure 7a-8a shows the modeled spatial distribution of near-surface daily mean ozone  
380 in spring 2008 over China from all natural and anthropogenic sources, i.e., the CTL  
381 case. Ozone concentrations reach 75–80 ppb over the southern Tibetan Plateau, and  
382 they are minimum (25–40 ppb) over the North China Plain and many populous cities

383 across eastern China. Ozone are about 45–60 ppb over the vast southeast, northwest  
384 and northeast.

385 The simulated natural ozone (i.e., without anthropogenic emissions worldwide, the  
386 xANTH case) shows a strong gradient from the southern Tibetan Plateau (65–75 ppb)  
387 to the northwest (35–40 ppb) and the east (20–35 ppb) (Fig. 7e8c). Wang et al. (2011)  
388 shows similar gradients of ~~nature-natural~~ ozone in 2006. Natural ozone contributes 80–  
389 90% of total surface ozone over Tibet and the northwest with low local anthropogenic  
390 emissions. The large natural ozone concentrations over Tibet are a result of vertical  
391 transport from the free troposphere and stratosphere due to its high altitudes and hilly  
392 terrains (that are conducive to vertical exchange) (Ding and Wang, 2006; Lin et al.,  
393 2015; Xu et al., 2017). They pose potential threats for public health and ecosystems  
394 there.

395 The simulated background ozone (i.e., without Chinese anthropogenic emissions, the  
396 xCH case) is shown in Fig. 7b8b. The background ozone ~~are-is~~ higher than the natural  
397 ozone by 2–11 ppb over most Chinese regions (Fig. 8b9b). This indicates large  
398 influences of foreign anthropogenic emissions through atmospheric transport of ozone  
399 and its precursors, as discussed in detail below.

#### 400 4.2 Domestic versus foreign anthropogenic contributions to ozone

401 Figure 8a-9a shows the spatial distribution of domestic anthropogenic contributions to  
402 daily mean surface ozone over China (~~difference between the control run and the~~  
403 ~~sensitivity simulation, CTL - xCH, adjusted with Eq. 1, followed by a linear~~  
404 ~~weighting adjustment~~). Over most of the west and northeast, Chinese anthropogenic  
405 emissions are relatively low, and they result in ozone concentrations by 0–4 ppb. In  
406 contrast, domestic contributions reach 16–25 ppb over the south due to more emissions  
407 and favorable conditions for photochemistry. Over the North China Plain and many  
408 populous cities, Chinese anthropogenic emissions lead to reductions (instead of  
409 enhancements) of surface ozone. This is because of a weak ozone production efficiency  
410 and a strong titration effect by excessive domestic NO<sub>x</sub> emissions. Figure 8d9d-f  
411 shows that when O<sub>x</sub> (= O<sub>3</sub> + NO<sub>2</sub>) is considered, Chinese anthropogenic contributions  
412 vary from 2–4 ppb over the west to 6–12 ppb over the North China Plain and to 20–35  
413 ppb over the southeast (Fig. 8d9d).

414 Figure 8b-9b shows the simulated contributions to Chinese surface ozone by all foreign  
415 anthropogenic emissions. Foreign contributions reach 7–11 ppb along much of Chinese  
416 borders, and they exceed 6 ppb over the vast northern regions. The foreign contribution  
417 reduces from the border to the inner areas, with a minimum (2–3 ppb) over the Sichuan  
418 Basin where the air is more isolated. In terms of anthropogenic ozone, foreign  
419 contributions account for up to 90% over most of western and northeastern China (Fig.  
420 8e9c), consistent with the findings by Li et al. (2015) for western China in 2000. Foreign  
421 anthropogenic contributions to O<sub>x</sub> over China are similar to their contributions to ozone  
422 (Fig. 8e9e), except at places with strong Chinese NO<sub>x</sub> emissions that lead to titration

423 of ozone.

424 Figure 9-10 further shows the contributions to Chinese surface ozone by anthropogenic  
425 emissions in seven individual foreign regions. The pattern of influence differs among  
426 these source regions due to differences in the location of source region, emission  
427 magnitude, pollutant lifetimes and transport pathways. Anthropogenic emissions in  
428 Japan and Korea result in 0.6–2.1 ppb of ozone enhancement along the Chinese coast.  
429 The tagged ozone simulation with NAQPMS by Li et al. (2016) also showed that about  
430 0.5–3.0 ppb of ozone over northeastern China in spring 2010 were produced over Korea  
431 peninsula, although there is a difference between ozone produced over a region and  
432 ozone produced from that region’s emissions. Emissions from South-East Asia  
433 contribute 1–5 ppb over much of the southern provinces. Emissions from South Asia  
434 mostly affect southwestern China and Tibet (by up to 5-10 ppb over the border), due to  
435 effective transport by strong southwesterly associated with the Indian Monsoon. The  
436 “Rest of Asia” consists of many countries to the west of China, whose total  
437 contributions are about 2–5 ppb over much of northwestern China.

438 European anthropogenic emissions contribute 2.1–3.0 ppb of ozone along the northern  
439 border of China. The contributions decrease southward, and are above 1 ppb over half  
440 of Chinese land areas. The [Model for Ozone and Related chemical Tracers \(MOZART\)](#)  
441 [simulation](#) by Li et al. (2015) also showed a European contribution by 2 ppb to surface  
442 ozone over North China in 2000. North American anthropogenic emissions increase  
443 ozone by 1.8–2.7 ppb over much of western China, by 1.5–2.1 ppb over the populous  
444 North China Plain, and by less than 0.9 ppb over the south. The contributions are  
445 smaller than springtime Asian anthropogenic influences on western North America  
446 (e.g., 1–5 ppb averaged over 2001–2005 (Brown-Steiner and Hess, 2011b)), although  
447 the affected population is larger by roughly an order of magnitude.

448 Influences from “Rest of World” are about 0.6–1.2 ppb over Tibet and smaller over  
449 other Chinese land territory. The larger values over Tibet reflect its higher altitude and  
450 greater sensitivity to long-range transport via the free troposphere.

451 [Figure 11a shows whether domestic or foreign anthropogenic contributions are higher](#)  
452 [at individual locations. Domestic anthropogenic contributions are higher than foreign](#)  
453 [contributions over southern China and parts of northern China. However, foreign](#)  
454 [anthropogenic contributions exceed domestic contributions over western China and](#)  
455 [most of the north, including the populated North China Plain. Over western China,](#)  
456 [foreign emissions contribute 70–90% of the total anthropogenic ozone.](#)

457 Figure 10a–11b further highlights the largest foreign contributor to surface  
458 anthropogenic ozone at each location of China. North America is the largest foreign  
459 contributor over about half of Chinese land territory, including the populated North  
460 China Plain. Europe is the largest foreign contributor for the vast northeastern region,  
461 Rest of Asia for the western border region, South Asia for southwestern China, South-  
462 East Asia for southern China, and Japan and Korea for the eastern coast of China.

463 4.3 Discussion of source attribution with an alternative 20% perturbation method, on  
464 extreme ozone, and on other years

465 The HTAP and several other studies have used 20% perturbation simulations (i.e.,  
466 reducing anthropogenic emissions in each source region by 20%) to study the  
467 transboundary ozone problem. Such studies are source-receptor analyses that are more  
468 relevant to the question of how much a modest cut in foreign emissions would reduce  
469 ozone pollution over a targeted receptor region. To compare with such a method, here  
470 we ran one more set of full chemistry simulations by decreasing 20% anthropogenic  
471 emissions over each of the eight emission source regions (see the detailed information  
472 in Table A2). We also applied the linear weighting method to account for the non-  
473 linearity of ozone chemistry. Figures 9a and 12a compare the Chinese anthropogenic  
474 contributed ozone calculated from zero-out and from 20%-perturbation simulations.  
475 Compared to the zero-out method, the 20% perturbation method leads to less Chinese  
476 contributed ozone, with negative values over more regions and smaller positive values  
477 over southern China. This result confirms our general finding that in spring 2008, the  
478 excessive domestic NO<sub>x</sub> emissions lead to relatively weak ozone production and/or  
479 strong ozone titration. Comparing with the zero-out method, the absolute foreign  
480 anthropogenic ozone obtained from 20%-perturbation simulations are smaller by 2–3  
481 ppb over the northern border of China (comparing Figs. 9b and 12b), whereas the  
482 percentage foreign contributions increase from 10–20% to 20–40% over southeastern  
483 China (comparing Fig 9c and 12c). Nonetheless, the spatial patterns are similar  
484 between the two methods for both the absolute and the relative foreign contributions.

485 As peak ozone is a critical problem for human health, here we show the domestic versus  
486 foreign contributions to modeled extreme ozone values in spring 2008 (defined as the  
487 average of the top 5% hourly ozone concentrations) (Fig. 12d–f). As expected, Chinese  
488 domestic contribution is larger for extreme ozone than for mean ozone; the negative  
489 values also disappear over North China Plain and Northeast China (comparing Fig. 9a  
490 and 12d). The absolute foreign contribution (in ppb) is also enhanced across China  
491 (comparing Fig. 9b and 12e). The percentage foreign contribution is within 10% over  
492 southern China, about 10–50% over the north, and above 70% over the west.  
493 Nevertheless, these results for extreme ozone should be interpreted with more caution,  
494 as the model cannot simulate the dates of extreme ozone very well (Fig. 4).

495 Previous studies have shown notable interannual variability in surface ozone over  
496 China driven by changes in precursor emissions and meteorology (Xu et al., 2008; Jin  
497 et al., 2015; Wang et al., 2017). To test how the interannual variability of meteorology  
498 and emissions would affect our source attribution findings, we have repeated all zero-  
499 out runs for spring 2012, the latest year when the GEOS-5 meteorological fields are  
500 available. Emissions for 2012 were adopted from the Community Emissions Data  
501 System (CEDS) inventory (Hoesly et al., 2018); 2012 is also the latest year the CEDS  
502 emissions for China are adjusted by the MEIC inventory. Table 5 shows the  
503 anthropogenic emissions in the two years. All zero-out simulation results in 2012  
504 underwent the same linear weighting adjustment as for those in 2008. Figure 12g–i

505 show the results for domestic versus foreign contributed ozone in spring 2012, as  
506 compared to the results for spring 2008 (Fig. 9a–c). In absolute terms, Chinese  
507 contributed ozone are similar between 2008 and 2012 (comparing Fig. 12g and Fig.  
508 9a), reflecting the slight changes in domestic precursor emissions (Table 5). From 2008  
509 to 2012, the absolute foreign contributed ozone increase along the southern boarder  
510 due to much enhanced emissions in South-East Asia and South Asia. The absolute  
511 foreign contributions decrease over the north and south, reflecting the net effect of  
512 changes in European and North American emissions (within 20% for both NO<sub>x</sub> and  
513 NM<sub>2</sub>VOC), increased emissions in Rest of Asia, and changes in meteorology. In relative  
514 terms (Figs. 9c and 12i), the percentage foreign anthropogenic contributions to total  
515 anthropogenic ozone decrease from 2008 to 2012 over southern China. Nonetheless,  
516 in both years the percentage foreign contributions exceed 50% over western China and  
517 are 5–40% over southern China. Therefore our general finding that both foreign and  
518 domestic contributions to Chinese anthropogenic ozone are important holds true for  
519 these two years.

## 520 **5. Vertical distributions of domestic and foreign anthropogenic contributions**

521 Figure ~~44a-13a~~ shows the domestic and foreign anthropogenic contributions to daily  
522 mean ozone at different heights above the ground averaged over China. The black line  
523 shows that Chinese emissions contribute 6.0–10.5 ppb of ozone below 2 km over China,  
524 with a maximum value at 0.7 km. This average amount of contribution reflects  
525 compensation between positive values over most regions and negative values over the  
526 North China Plain and many populous cities (see Sect. 4.2). Above 0.7 km, Chinese  
527 contribution decreases rapidly until 3 ppb at 5 km, above which height the contribution  
528 declines slowly until a value at 1 ppb at 12 km. By comparison, Chinese contribution  
529 to Ox is about 7–11 ppb below 2 km, and at higher altitudes the contribution is almost  
530 identical to that for ozone (not shown). The small contributions above 2 km for both  
531 ozone and Ox are because as ozone and precursors associated with Chinese emissions  
532 are lifted to higher altitudes, they are transported out of Chinese territory and destroyed  
533 gradually.

534 The grey line in Fig. ~~44a-13a~~ shows that the total foreign contribution is about 5.2–7.8  
535 ppb at different heights with a reverse “C” shape, i.e., higher values at 3–9 km and  
536 lower values above or below that layer. The foreign contribution exceeds Chinese  
537 contribution at all heights above 2 km. Nonetheless, the total (Chinese + foreign)  
538 anthropogenic ozone is less than one third of natural ozone throughout the troposphere.  
539 Figure ~~40b-11c~~ shows that of ozone over China produced from all anthropogenic  
540 emissions, foreign emissions together contribute 50% at the surface, 40% at 0.7 km as  
541 a minimum, and 85% in the upper troposphere.

542 Figure ~~44b-13b~~ specifies the contribution of each foreign emission source region. Figure  
543 ~~44e-13c~~ further separates the portion of ozone produced within each source region’s  
544 territory from the portion produced outside of that source region; results here were  
545 derived from a combination of zero-out simulations (e.g., CTL and xEU) and tagged

§46 [simulations \(e.g., T\\_CTL and T\\_xEU\)](#). South-East Asian contribution is about 0.5–2.5  
547 ppb averaged over China, and it increases with height due to strong upwelling that lifts  
548 pollutants to the middle and upper troposphere. The contribution from Japan and Korea  
§49 is below 0.5 ppb throughout the troposphere averaged over China (Fig. [Hb13b](#)). The  
550 share of transboundary ozone produced within South-East Asian territory and  
551 transported to China is about 10–45% (mostly below 30%), and the share for ozone  
§52 produced within Japan and Korea is even smaller (5–25%) (Fig. [He13c](#)), highlighting  
553 the importance of ozone produced by precursors transported out of these two emission  
554 source regions.

555 South Asian contribution is only about 0.5–1.2 ppb throughout the troposphere (Fig.  
§56 [Hb13b](#)). Although South Asia has more anthropogenic emissions than South-East Asia  
557 (Table 2), its contribution to ozone over China is smaller due to blocking of transport  
§58 by the Himalayas with high elevation (Fig. [23](#)). In addition, the share of transboundary  
559 ozone produced within South Asian territory reaches 70–90% below 6 km but declines  
§60 rapidly to 28% at 12 km (Fig. [He13c](#)), a characteristic drastically different from the  
561 share for South-East Asia.

562 The contribution from Rest of Asia is below 1.8 ppb at all heights with a negative  
§63 vertical gradient (Fig. [Hb13b](#)). Above 3 km, the portion of transboundary ozone  
564 produced within the territory of Rest of Asia is similar to that for South Asia (Fig.  
§65 [He13c](#)). However, the portion exhibits a strong vertical gradient below 3 km, with a  
566 minimum value at 45% near the ground.

567 European contribution declines from 1.5 ppb in the lower troposphere to 0.2 ppb at 12  
§68 km, similar to that for Rest of Asia (Fig. [Hb13b](#)). In spring, Eurasian frontal activities  
569 transport and gradually lift European pollutants to downwind areas. The portion of  
570 transboundary ozone produced within European territory is about 55–65% at 3–10 km  
§71 but is as low as 20% below 1 km (Fig. [He13c](#)), suggesting that most Europe-  
572 contributed near-surface ozone over China are produced from precursors transported  
573 out of Europe.

§74 Figure [Hb-13b](#) shows that North American anthropogenic emissions contribute about  
575 1.5–2.5 ppb of ozone below 8 km, although the contribution declines rapidly to 0.2 ppb  
576 at 12 km. Compared to Europe, North America is further away from China, but its  
577 pollutants can be transported via the strong mid-latitude westerly. Averaged over China,  
578 North American contribution is larger than European contribution at all heights, e.g.,  
579 by a factor of two in the middle and upper troposphere. The higher contribution is due  
580 to much more anthropogenic emissions in North America than in Europe. Table 3 shows  
581 that North America emits NMVOC nearly twice as much as Europe does; and Wu et al.  
582 (2009) showed that the amount of transboundary ozone is nearly proportional to  
§83 NMVOC emissions of the source region. In addition, Fig. [He-13c](#) shows that the  
584 portion of transboundary ozone produced within North American territory is only about  
585 5–20% below 8 km, reflecting the dominant contribution by ozone produced from  
586 transported precursors. The low share of ozone produced within North America is

587 primarily because most of such ozone is destroyed during the transport from North  
588 America to China (for about two weeks), given the tropospheric lifetime of ozone at  
589 about three weeks (Yan et al., 2016).

590 The grey line in Fig. ~~He-13c~~ shows the average portion of transboundary ozone from  
591 all foreign source regions that is produced within the territories of respective foreign  
592 regions. The average portion is less than 50% throughout the troposphere, is about 40%  
593 at 2 km, and is as low as 25% near the surface. This again highlights the dominant  
594 importance of ozone production along with the transport of precursors.

595 Figure 14 further shows the vertical profiles of ozone from different sources averaged  
596 over regions where Chinese anthropogenic emissions contribute more surface ozone  
597 than total foreign anthropogenic emissions (i.e., southern China, Fig. 14a, b), as well as  
598 averaged over regions where foreign anthropogenic emissions dominate (Fig. 14c, d).  
599 Even over areas where domestic contributions to near-surface ozone exceed total  
600 foreign contributions, the regional average ozone contributed by foreign emissions  
601 exceeds those contributed by domestic emissions above 3.5 km (Fig. 14a). Figure 14b  
602 and d further shows that the (relative) vertical shape of regional average ozone  
603 contributed by each foreign source region is similar to the shape of China averaged  
604 results in Fig. 13b, although the absolute values (in ppb) are different.

## 605 **6. Conclusions**

606 This study uses a GEOS-Chem based two-way coupled modeling system to simulate  
607 Chinese and foreign anthropogenic contributions to springtime ozone at different  
608 heights over China. Anthropogenic contributions are associated with anthropogenic  
609 NO<sub>x</sub>, CO and NMVOC emissions, excluding the effect of methane. We combine the  
610 zero-out simulations and tagged ozone simulations to separate the transboundary ozone  
611 produced within the territory of each emission source region from the ozone produced  
612 by anthropogenic precursors transported out of that source region. We use a weighting  
613 approach to accounting for the effect of nonlinear ozone chemistry on source attribution  
614 estimates. Model evaluation using a suite of ground, aircraft and ozonesonde  
615 measurements show an overall small bias for ozone near the surface and in the  
616 troposphere (10% at 10 surface sites with hourly measurements, 15% at 21 surface sites  
617 with monthly observations, and 12% for vertical profiles). The model underestimates  
618 CO by 20% on average over China and nearby areas, which however does not affect  
619 the simulated ozone significantly.

620 Model simulations reveal that both total and natural ozone near the surface over China  
621 show a decreasing gradient from the southern Tibetan Plateau to the northwest and the  
622 east. Natural ozone contributes 80–90% of total surface ozone over Tibet and the  
623 northwest with low local anthropogenic emissions. Chinese anthropogenic emissions  
624 enhance surface ozone concentrations by 0–4 ppb over most of the west and northeast  
625 due to low emissions and by 16–25 ppb over the south due to more emissions and  
626 chemically conducive conditions. Chinese anthropogenic emissions result in reduced

627 ozone, albeit with enhanced Ox, over the North China Plain and many populous cities,  
628 as a result of weak ozone production efficiency and strong titration by excessive  
629 Chinese NOx emissions.

630 Near the surface, foreign anthropogenic emissions contribute 2–11 ppb of Chinese  
631 ozone, with peak contributions at 7–11 ppb over the border and coastal regions of China.  
632 Over western and northeastern China, foreign emissions account for up to 90% of ozone  
633 of anthropogenic origin. Anthropogenic emissions in Japan and Korea result in 0.6–2.1  
634 ppb of ozone along the Chinese coast. Emissions in South-East Asia contribute 1–5 ppb  
635 over much of southeastern China. South Asian emissions mostly affect southwestern  
636 China and Tibet (by up to 5 ppb), due to effective transport by strong southwesterly  
637 associated with the Indian Monsoon. European anthropogenic emissions contribute  
638 2.1–3 ppb along the northern border of China and the contribution decreases southwards.  
639 North American anthropogenic emissions increase ozone by 1.8–2.7 ppb over much of  
640 the west, by 1.5–2.1 ppb over the populous North China Plain, and by less than 0.9 ppb  
641 over the south.

642 Vertically, for ozone of anthropogenic origin averaged over China, Chinese emissions  
643 contribute ~ 6 ppb (50%) of ozone at the surface, 6.0–10.5 ppb below 2 km, decreasing  
644 to 3 ppb at 5 km and 1 ppb at 12 km. The total foreign contribution increases from 40–  
645 50% below 2 km to 50–85% above that height. The contribution from Japan and Korea  
646 is below 0.5 ppb throughout the troposphere averaged over China. Despite its large  
647 emissions, South Asia contributes only about 0.5–1.2 ppb throughout the troposphere  
648 due to blocking of transport by the Himalayas. South-East Asian contribution increases  
649 with height due to strong upwelling that lifts pollutants to the upper troposphere. On  
650 the contrary, European contributions decreases from 1.5 ppb in the lower troposphere  
651 to 0.2 ppb at 12 km. Despite the long transport distance, North American contribution  
652 reaches as much as 1.5–2.5 ppb below 8 km due to its large anthropogenic emissions  
653 and the strong mid-latitude westerly favorable for transboundary transport.

654 For ozone of foreign anthropogenic origin averaged over China, the portion of  
655 transboundary ozone produced within foreign source regions is less than 50%  
656 throughout the troposphere, albeit with a strong vertical variability, indicating the  
657 importance of ozone produced by precursors transported out of those source regions.  
658 The portion also differs among each foreign source region of South-East Asia (10–45%)  
659 and Japan and Korea (5–25%), South Asia (from 70–90% below 6 km to 28% at 12  
660 km), Europe (from 20% below 1 km to 55–65% at 3–10 km), and North America (5–  
661 20% below 8 km). Thus, tracing ozone produced within the territory of a particular  
662 region is drastically different from tracing ozone associated with emissions in that  
663 region.

664 In summary, although China is a major pollutant emitter, the ozone above its territory  
665 consists primarily of natural sources, especially over western China with low local  
666 anthropogenic emissions. Moreover, for ozone of anthropogenic origin, a large portion  
667 results from foreign emissions, as analyzed here for spring 2008. In more recent years,

668 Chinese anthropogenic NO<sub>x</sub> emissions have undergone a rapid decline as a result of  
669 domestic emission control (Xia et al., 2016), along with continuous reductions in North  
670 America and Western Europe (Yan et al., 2017a, 2018a; 2017b, 2018b) and changes in  
671 other regions. Future research is needed to quantify the resulting changes in ozone and  
672 its geographical origin. In addition, this study does not account for that a substantial  
673 portion of anthropogenic emissions in any region are associated with economic  
674 production for foreign consumption (Lin et al., 2014; Jiang et al., 2015a), which would  
675 affect how pollution is attributed to individual producing or consuming regions (Guan  
676 et al., 2014; Lin et al., 2016; Zhang et al., 2017). Nevertheless, our study suggests the  
677 great importance of global collaboration on emission reduction to mitigate ozone  
678 pollution in addition to domestic emission control efforts.

## 679 **Acknowledgments**

680 This research is supported by the National Natural Science Foundation of China  
681 (41775115) and the 973 program (2014CB441303). We acknowledge Dr. Chen  
682 Hongbin's team at IAP LAGEO for providing the GPSO3 ozonesonde data. We  
683 acknowledge the free use of ozone data from WDCGG  
684 (<http://ds.data.jma.go.jp/gmd/wdcgg/>), EANET  
685 (<http://www.eanet.asia/product/index.html>), WOUDC  
686 (<http://www.woudc.org/data/explore.php?lang=en>), and MOZAIC-IAGOS  
687 (<http://www.iagos.fr/web/>). We thank the European Commission for the support to the  
688 MOZAIC project (1994–2003) and the preparatory phase of IAGOS (2005–2012)  
689 partner institutions of the IAGOS Research Infrastructure (FZJ, DLR, MPI, KIT in  
690 Germany, CNRS, CNES, Météo-France in France and University of Manchester in  
691 United Kingdom), ETHER (CNES-CNRS/INSU) for hosting the database, the  
692 participating airlines (Lufthansa, Air France, Austrian, China Airlines, Iberia, Cathay  
693 Pacific) for the transport free of charge of the instrumentation.

## 694 **References**

- 695 Auvray, M., and Bey, I.: Long-range transport to Europe: Seasonal variations and  
696 implications for the European ozone budget, *J. Geophys. Res.-Atmos.*, 110,  
697 10.1029/2004jd005503, 2005.
- 698 Bian, J. C., Gettelman, A., Chen, H. B., and Pan, L. L.: Validation of satellite ozone  
699 profile retrievals using Beijing ozonesonde data, *J. Geophys. Res.-Atmos.*, 112,  
700 11, 10.1029/2006jd007502, 2007.
- 701 Bond, T. C., Bhardwaj, E., Dong, R., Jogani, R., Jung, S., Roden, C., Streets, D. G.,  
702 and Trautmann, N. M.: Historical emissions of black and organic carbon aerosol  
703 from energy-related combustion, 1850–2000, *Global Biogeochem. Cy.*, 21,  
704 GB2018, doi:10.1029/2006GB002840, 2007.
- 705 Brown-Steiner, B., and Hess, P.: Asian influence on surface ozone in the United States:  
706 A comparison of chemistry, seasonality, and transport mechanisms, *J. Geophys.*  
707 *Res.-Atmos.*, 116, 13, 10.1029/2011jd015846, 2011.

708 Cooper, O. R., Parrish, D. D., Stohl, A., Trainer, M., Nedelec, P., Thouret, V., Cammas,  
709 J. P., Oltmans, S. J., Johnson, B. J., Tarasick, D., Leblanc, T., McDermid, I. S.,  
710 Jaffe, D., Gao, R., Stith, J., Ryerson, T., Aikin, K., Campos, T., Weinheimer, A.,  
711 and Avery, M. A.: Increasing springtime ozone mixing ratios in the free  
712 troposphere over western North America, *Nature*, 463, 344-348,  
713 10.1038/nature08708, 2010.

714 Derwent, R. G., Stevenson, D. S., Collins, W. J., and Johnson, C. E.: Intercontinental  
715 transport and the origins of the ozone observed at surface sites in Europe,  
716 *Atmospheric Environment*, 38, 1891-1901, 10.1016/j.atmosenv.2004.01.008,  
717 2004.

718 Ding, A. J., and Wang, T.: Influence of stratosphere-to-troposphere exchange on the  
719 seasonal cycle of surface ozone at Mount Waliguan in western China, *Geophysical*  
720 *Research Letters*, 33, 4, 10.1029/2005gl024760, 2006.

721 Fang, S. X., Zhou, L. X., Tans, P. P., Ciais, P., Steinbacher, M., Xu, L., and Luan, T.:  
722 In situ measurement of atmospheric CO<sub>2</sub> at the four WMO/GAW stations in China,  
723 *Atmospheric Chemistry and Physics*, 14, 2541-2554, 10.5194/acp-14-2541-2014,  
724 2014.

725 Guan, D., Su, X., Zhang, Q., Peters, G. P., Liu, Z., Lei, Y., and He, K.: The  
726 socioeconomic drivers of China's primary PM<sub>2.5</sub> emissions, *Environmental*  
727 *Research Letters*, 9, 024010, 2014.

728 Geng, G. N., Zhang, Q., Martin, R. V., Lin, J. T., Huo, H., Zheng, B., Wang, S. W., and  
729 He, K. B.: Impact of spatial proxies on the representation of bottom-up emission  
730 inventories: A satellite-based analysis, *Atmospheric Chemistry and Physics*, 17,  
731 4131-4145, 10.5194/acp-17-4131-2017, 2017.

732 Guenther, A. B., Jiang, X., Heald, C. L., Sakulyanontvittaya, T., Duhl, T., Emmons, L.  
733 K., and Wang, X.: The Model of Emissions of Gases and Aerosols from Nature  
734 version 2.1 (MEGAN2.1): an extended and updated framework for modeling  
735 biogenic emissions, *Geoscientific Model Development*, 5, 1471-1492,  
736 10.5194/gmd-5-1471-2012, 2012.

737 [Hoesly, R. M., Smith, S. J., Feng, L., Klimont, Z., Janssens-Maenhout, G., Pitkanen, T.,](#)  
738 [Seibert, J. J., Vu, L., Andres, R. J., Bolt, R. M., Bond, T. C., Dawidowski, L.,](#)  
739 [Kholod, N., Kurokawa, J.-I., Li, M., Liu, L., Lu, Z., Moura, M. C. P., O'Rourke,](#)  
740 [P. R., and Zhang, Q.: Historical \(1750–2014\) anthropogenic emissions of reactive](#)  
741 [gases and aerosols from the Community Emissions Data System \(CEDS\), \*Geosci.\*](#)  
742 [Model Dev., 11, 369-408, <https://doi.org/10.5194/gmd-11-369-2018>, 2018](#)

743 Holtzlag, A. A. M., and Boville, B. A.: LOCAL VERSUS NONLOCAL BOUNDARY-  
744 LAYER DIFFUSION IN A GLOBAL CLIMATE MODEL, *Journal of Climate*,  
745 6, 1825-1842, 10.1175/1520-0442(1993)006<1825:lvnbld>2.0.co;2, 1993.

746 HTAP: Hemispheric Transport of Air Pollution 2010 Executive Summary  
747 ECE/EB.AIR/2010/10 Corrected, United Nations, available at:  
748 [http://www.htap.org/publications/2010\\_report/2010\\_Final\\_Report/EBMeeting20](http://www.htap.org/publications/2010_report/2010_Final_Report/EBMeeting20)  
749 [10.pdf](#) (last access: 1 February 2015), 2010.

750 Hudman, R. C., Moore, N. E., Mebust, A. K., Martin, R. V., Russell, A. R., Valin, L.  
751 C., and Cohen, R. C.: Steps towards a mechanistic model of global soil nitric oxide

752 emissions: implementation and space based-constraints, *Atmospheric Chemistry*  
753 *and Physics*, 12, 7779-7795, 10.5194/acp-12-7779-2012, 2012.

754 Jacob, D. J., Logan, J. A., and Murti, P. P.: Effect of rising Asian emissions on surface  
755 ozone in the United States, *Geophysical Research Letters*, 26, 2175-2178,  
756 10.1029/1999gl900450, 1999.

757 Jiang, X., Zhang, Q., Zhao, H., Geng, G., Peng, L., Guan, D., Kan, H., Huo, H., Lin, J.-  
758 T., Brauer, M., Martin, R. V., and He, K.: Revealing the hidden health costs  
759 embodied in Chinese exports, *Environmental Science & Technology*,  
760 10.1021/es506121s, 2015a.

761 Jiang, Z., Worden, J. R., Jones, D. B. A., Lin, J. T., Verstraeten, W. W., and Henze, D.  
762 K.: Constraints on Asian ozone using Aura TES, OMI and Terra MOPITT,  
763 *Atmospheric Chemistry and Physics*, 15, 99-112, 10.5194/acp-15-99-2015, 2015b.

764 Jiang, Z., Worden, J. R., Payne, V. H., Zhu, L. Y., Fischer, E., Walker, T., and Jones,  
765 D. B. A.: Ozone export from East Asia: The role of PAN, *J. Geophys. Res.-Atmos.*,  
766 121, 6555-6563, 10.1002/2016jd024952, 2016.

767 [Jin, X., and Holloway, T.: Spatial and temporal variability of ozone sensitivity over](#)  
768 [China observed from the Ozone Monitoring Instrument, \*J. Geophys. Res. Atmos.\*,](#)  
769 [120, 7229–7246, doi:10.1002/2015JD023250, 2015.](#)

770 Kuhns, H., Knipping, E. M., and Vukovich, J. M.: Development of a United States-  
771 Mexico emissions inventory for the Big Bend Regional Aerosol and Visibility  
772 Observational (BRAVO) Study, *Journal of the Air & Waste Management*  
773 *Association*, 55, 677-692, 2005.

774 Kopacz, M., Jacob, D. J., Fisher, J. A., Logan, J. A., Zhang, L., Megretskaja, I. A.,  
775 Yantosca, R. M., Singh, K., Henze, D. K., Burrows, J. P., Buchwitz, M., Khlystova,  
776 I., McMillan, W. W., Gille, J. C., Edwards, D. P., Eldering, A., Thouret, V., and  
777 Nedelec, P.: Global estimates of CO sources with high resolution by adjoint  
778 inversion of multiple satellite datasets (MOPITT, AIRS, SCIAMACHY, TES),  
779 *Atmospheric Chemistry and Physics*, 10, 855-876, 2010.

780 Li, B. G., Gasser, T., Ciais, P., Piao, S. L., Tao, S., Balkanski, Y., Hauglustaine, D.,  
781 Boisier, J. P., Chen, Z., Huang, M. T., Li, L. Z., Li, Y., Liu, H. Y., Liu, J. F., Peng,  
782 S. S., Shen, Z. H., Sun, Z. Z., Wang, R., Wang, T., Yin, G. D., Yin, Y., Zeng, H.,  
783 Zeng, Z. Z., and Zhou, F.: The contribution of China's emissions to global climate  
784 forcing, *Nature*, 531, 357-361, 10.1038/nature17165, 2016a.

785 Li, J., Yang, W. Y., Wang, Z. F., Chen, H. S., Hu, B., Li, J. J., Sun, Y. L., Fu, P. Q.,  
786 and Zhang, Y. Q.: Modeling study of surface ozone source-receptor relationships  
787 in East Asia, *Atmospheric Research*, 167, 77-88, 10.1016/j.atmosres.2015.07.010,  
788 2016b.

789 Li, M., Zhang, Q., Kurokawa, J., Woo, J. H., He, K. B., Lu, Z. F., Ohara, T., Song, Y.,  
790 Streets, D. G., Carmichael, G. R., Cheng, Y. F., Hong, C. P., Huo, H., Jiang, X. J.,  
791 Kang, S. C., Liu, F., Su, H., and Zheng, B.: MIX: a mosaic Asian anthropogenic  
792 emission inventory under the international collaboration framework of the MICS-  
793 Asia and HTAP, *Atmospheric Chemistry and Physics*, 17, 935-963, 10.5194/acp-  
794 17-935-2017, 2017.

795 Li, X. Y., Liu, J. F., Mauzerall, D. L., Emmons, L. K., Walters, S., Horowitz, L. W.,  
796 and Tao, S.: Effects of trans-Eurasian transport of air pollutants on surface ozone  
797 concentrations over Western China, *J. Geophys. Res.-Atmos.*, 119, 12338-12354,  
798 10.1002/2014jd021936, 2014.

799 Liang, Q., Jaegle, L., Jaffe, D. A., Weiss-Penzias, P., Heckman, A., and Snow, J. A.:  
800 Long-range transport of Asian pollution to the northeast Pacific: Seasonal  
801 variations and transport pathways of carbon monoxide, *J. Geophys. Res.-Atmos.*,  
802 109, 20, 10.1029/2003jd004402, 2004.

803 Lin, J.-T., Wuebbles, D. J., and Liang, X.-Z.: Effects of intercontinental transport on  
804 surface ozone over the United States: Present and future assessment with a global  
805 model, *Geophysical Research Letters*, 35, 10.1029/2007gl031415, 2008.

806 Lin, J.-T., Pan, D., Davis, S. J., Zhang, Q., He, K., Wang, C., Streets, D. G., Wuebbles,  
807 D. J., and Guan, D.: China's international trade and air pollution in the United  
808 States, *Proceedings of the National Academy of Sciences*, 111, 1736-1741,  
809 10.1073/pnas.1312860111, 2014.

810 Lin, J. T., and McElroy, M. B.: Impacts of boundary layer mixing on pollutant vertical  
811 profiles in the lower troposphere: Implications to satellite remote sensing,  
812 *Atmospheric Environment*, 44, 1726-1739, 10.1016/j.atmosenv.2010.02.009,  
813 2010.

814 Lin, J. T., Liu, Z., Zhang, Q., Liu, H., Mao, J., and Zhuang, G.: Modeling uncertainties  
815 for tropospheric nitrogen dioxide columns affecting satellite-based inverse  
816 modeling of nitrogen oxides emissions, *Atmospheric Chemistry and Physics*, 12,  
817 12255-12275, 10.5194/acp-12-12255-2012, 2012a.

818 Lin, J. T., Tong, D., Davis, S., Ni, R. J., Tan, X. X., Pan, D., Zhao, H. Y., Lu, Z. F.,  
819 Streets, D., Feng, T., Zhang, Q., Yan, Y. Y., Hu, Y. Y., Li, J., Liu, Z., Jiang, X. J.,  
820 Geng, G. N., He, K. B., Huang, Y., and Guan, D. B.: Global climate forcing of  
821 aerosols embodied in international trade, *Nature Geoscience*, 9, 790-794,  
822 10.1038/ngeo2798, 2016.

823 Lin, M., Fiore, A. M., Horowitz, L. W., Cooper, O. R., Naik, V., Holloway, J., Johnson,  
824 B. J., Middlebrook, A. M., Oltmans, S. J., Pollack, I. B., Ryerson, T. B., Warner,  
825 J. X., Wiedinmyer, C., Wilson, J., and Wyman, B.: Transport of Asian ozone  
826 pollution into surface air over the western United States in spring, *J. Geophys.*  
827 *Res.-Atmos.*, 117, D00v07, 10.1029/2011jd016961, 2012b.

828 Lin, W., Xu, X., Zheng, X., Dawa, J., Baima, C., and Ma, J.: Two-year measurements  
829 of surface ozone at Dangxiong, a remote highland site in the Tibetan Plateau,  
830 *Journal of Environmental Sciences*, 31, 133-145,  
831 <https://doi.org/10.1016/j.jes.2014.10.022>, 2015.

832 Lin, W. L., Xu, X. B., Ge, B. Z., and Zhang, X. C.: Characteristics of gaseous pollutants  
833 at Gucheng, a rural site southwest of Beijing, *J. Geophys. Res.-Atmos.*, 114, 17,  
834 10.1029/2008jd010339, 2009.

835 Liu, Z., Wang, Y. H., Gu, D. S., Zhao, C., Huey, L. G., Stickel, R., Liao, J., Shao, M.,  
836 Zhu, T., Zeng, L. M., Liu, S. C., Chang, C. C., Amoroso, A., and Costabile, F.:  
837 Evidence of Reactive Aromatics As a Major Source of Peroxy Acetyl Nitrate over

838 China, *Environmental Science & Technology*, 44, 7017-7022, 10.1021/es1007966,  
839 2010.

840 Ma, J., Lin, W. L., Zheng, X. D., Xu, X. B., Li, Z., and Yang, L. L.: Influence of air  
841 mass downward transport on the variability of surface ozone at Xianggelila  
842 Regional Atmosphere Background Station, southwest China, *Atmospheric  
843 Chemistry and Physics*, 14, 5311-5325, 10.5194/acp-14-5311-2014, 2014.

844 Mao, J. Q., Paulot, F., Jacob, D. J., Cohen, R. C., Crouse, J. D., Wennberg, P. O.,  
845 Keller, C. A., Hudman, R. C., Barkley, M. P., and Horowitz, L. W.: Ozone and  
846 organic nitrates over the eastern United States: Sensitivity to isoprene chemistry,  
847 *J. Geophys. Res.-Atmos.*, 118, 11256-11268, 10.1002/jgrd.50817, 2013.

848 Marenco, A., Thouret, V., Nedelec, P., Smit, H., Helten, M., Kley, D., Karcher, F.,  
849 Simon, P., Law, K., Pyle, J., Poschmann, G., Von Wrede, R., Hume, C., and Cook,  
850 T.: Measurement of ozone and water vapor by Airbus in-service aircraft: The  
851 MOZAIC airborne program, An overview, *J. Geophys. Res.-Atmos.*, 103, 25631-  
852 25642, 10.1029/98jd00977, 1998.

853 McLinden, C. A., Olsen, S. C., Hannegan, B., Wild, O., Prather, M. J., and Sundet, J.:  
854 Stratospheric ozone in 3-D models: A simple chemistry and the cross-tropopause  
855 flux, *J. Geophys. Res.-Atmos.*, 105, 14653-14665, 10.1029/2000jd900124, 2000.

856 Moorthi, S., and Suarez, M. J.: Relaxed Arakawa-Schubert. A Parameterization of  
857 Moist Convection for General Circulation Models, *Monthly Weather Review*, 120,  
858 978-1002, 1992.

859 Murray, L. T., Jacob, D. J., Logan, J. A., Hudman, R. C., and Koshak, W. J.: Optimized  
860 regional and interannual variability of lightning in a global chemical transport  
861 model constrained by LIS/OTD satellite data, *J. Geophys. Res.-Atmos.*, 117, 14,  
862 10.1029/2012jd017934, 2012.

863 Ott, L. E., Pickering, K. E., Stenchikov, G. L., Allen, D. J., DeCaria, A. J., Ridley, B.,  
864 Lin, R. F., Lang, S., and Tao, W. K.: Production of lightning NO<sub>x</sub> and its vertical  
865 distribution calculated from three-dimensional cloud-scale chemical transport  
866 model simulations, *J. Geophys. Res.-Atmos.*, 115, 19, 10.1029/2009jd011880,  
867 2010.

868 Simone, N. W., Stettler, M. E. J., and Barrett, S. R. H.: Rapid estimation of global  
869 civil aviation emissions with uncertainty quantification, *Transport. Res. D-Tr. E.*,  
870 25, 33–41, doi:10.1016/j.trd.2013.07.001, 2013.

871 [Tu, J., Xia, Z., Wang, H., Li, W.: Temporal variations in surface ozone and its](#)  
872 [precursors and meteorological effects at an urban site in China, \*Atmos. Res.\* 85,](#)  
873 [310–337, 10.1016/j.atmosres.2007.02.003, 2007.](#)

874 van der Werf, G. R., Randerson, J. T., Giglio, L., Collatz, G. J., Mu, M., Kasibhatla, P.  
875 S., Morton, D. C., DeFries, R. S., Jin, Y., and van Leeuwen, T. T.: Global fire  
876 emissions and the contribution of deforestation, savanna, forest, agricultural, and  
877 peat fires (1997-2009), *Atmospheric Chemistry and Physics*, 10, 11707-11735,  
878 10.5194/acp-10-11707-2010, 2010.

879 Verstraeten, W. W., Neu, J. L., Williams, J. E., Bowman, K. W., Worden, J. R., and  
880 Boersma, K. F.: Rapid increases in tropospheric ozone production and export from

881 China (vol 8, pg 690, 2015), *Nature Geoscience*, 9, 643-643, 10.1038/ngeo2768,  
882 2016.

883 [Wang, W., Cheng, T., Gu, X., Chen, H., Guo, H., Wang, Y., Bao, F., Shi, S., Xu, B.,](#)  
884 [Zuo, X., Meng, C., and Zhang, X.: Assessing spatial and temporal patterns of](#)  
885 [observed ground-level ozone in China, \*Sci. Rep.\*, 7, 3651, 10.1038/s41598-017-](#)  
886 [03929-w, 2017.](#)

887 Wang, T., Ding, A. J., Gao, J., and Wu, W. S.: Strong ozone production in urban plumes  
888 from Beijing, China, *Geophysical Research Letters*, 33, 5, 10.1029/2006gl027689,  
889 2006.

890 Wang, Y., Zhang, Y., Hao, J., and Luo, M.: Seasonal and spatial variability of surface  
891 ozone over China: contributions from background and domestic pollution,  
892 *Atmospheric Chemistry and Physics*, 11, 3511-3525, 10.5194/acp-11-3511-2011,  
893 2011.

894 Wang, Y., Konopka, P., Liu, Y., Chen, H., Muller, R., Ploger, F., Riese, M., Cai, Z.,  
895 and Lu, D.: Tropospheric ozone trend over Beijing from 2002-2010: ozonesonde  
896 measurements and modeling analysis, *Atmospheric Chemistry and Physics*, 12,  
897 8389-8399, 10.5194/acp-12-8389-2012, 2012.

898 Wang, Y. H., Jacob, D. J., and Logan, J. A.: Global simulation of tropospheric O-3-  
899 NOx-hydrocarbon chemistry 1. Model formulation, *J. Geophys. Res.-Atmos.*, 103,  
900 10713-10725, 10.1029/98jd00158, 1998.

901 Wu, R. R., Bo, Y., Li, J., Li, L. Y., Li, Y. Q., and Xie, S. D.: Method to establish the  
902 emission inventory of anthropogenic volatile organic compounds in China and its  
903 application in the period 2008-2012, *Atmospheric Environment*, 127, 244-254,  
904 10.1016/j.atmosenv.2015.12.015, 2016.

905 Wu, S. L., Duncan, B. N., Jacob, D. J., Fiore, A. M., and Wild, O.: Chemical  
906 nonlinearities in relating intercontinental ozone pollution to anthropogenic  
907 emissions, *Geophysical Research Letters*, 36, 5, 10.1029/2008gl036607, 2009.

908 Xia, Y. M., Zhao, Y., and Nielsen, C. P.: Benefits of of China's efforts in gaseous  
909 pollutant control indicated by the bottom-up emissions and satellite observations  
910 2000-2014, *Atmospheric Environment*, 136, 43-53,  
911 10.1016/j.atmosenv.2016.04.013, 2016.

912 Xu, W., Lin, W., Xu, X., Tang, J., Huang, J., Wu, H., and Zhang, X.: Long-term trends  
913 of surface ozone and its influencing factors at the Mt Waliguan GAW station,  
914 China – Part 1: Overall trends and characteristics, *Atmos. Chem. Phys.*, 16, 6191-  
915 6205, 10.5194/acp-16-6191-2016, 2016.

916 Xu, W., Lin, W., Xu, X., Tang, J., Huang, J., Wu, H., and Zhang, X.: Long-term trends  
917 of surface ozone and its influencing factors at the Mt Waliguan GAW station,  
918 China – Part 1: Overall trends and characteristics, *Atmos. Chem. Phys.*, 16, 6191-  
919 6205, <https://doi.org/10.5194/acp-16-6191-2016>, 2016.

920 Xu, X., Lin, W., Wang, T., Yan, P., Tang, J., Meng, Z., and Wang, Y.: Long-term trend  
921 of surface ozone at a regional background station in eastern China 1991-2006:  
922 enhanced variability, *Atmospheric Chemistry and Physics*, 8, 2595-2607, 2008.

923 Xue, L. K., Wang, T., Zhang, J. M., Zhang, X. C., Deliger, Poon, C. N., Ding, A. J.,  
924 Zhou, X. H., Wu, W. S., Tang, J., Zhang, Q. Z., and Wang, W. X.: Source of

925 surface ozone and reactive nitrogen speciation at Mount Waliguan in western  
926 China: New insights from the 2006 summer study, *Journal of Geophysical*  
927 *Research: Atmospheres*, 116, n/a-n/a, 10.1029/2010JD014735, 2011.

928 Xue, L. K., Wang, T., Gao, J., Ding, A. J., Zhou, X. H., Blake, D. R., Wang, X. F.,  
929 Saunders, S. M., Fan, S. J., Zuo, H. C., Zhang, Q. Z., and Wang, W. X.: Ground-  
930 level ozone in four Chinese cities: precursors, regional transport and  
931 heterogeneous processes, *Atmospheric Chemistry and Physics*, 14, 13175-13188,  
932 10.5194/acp-14-13175-2014, 2014.

933 Yan, Y., Lin, J., Chen, J., and Hu, L.: Improved simulation of tropospheric ozone by a  
934 global-multi-regional two-way coupling model system, *Atmospheric Chemistry*  
935 *and Physics*, 16, 2381-2400, 10.5194/acp-16-2381-2016, 2016.

936 [Yan, Y., Lin, J., and He, C.: Ozone trends over the United States at different times of](#)  
937 [day, \*Atmos. Chem. Phys.\*, 18, 1185–1202, 10.5194/acp-18-1185-2018, 2018.](#)

938 [Yan, Y., Pozzer, A., Ojha, N., Lin, J., and Lelieveld, J.: Analysis of European ozone](#)  
939 [trends in the period 1995–2014, \*Atmos. Chem. Phys.\*, 18, 5589–5605,](#)  
940 [10.5194/acp-18-5589-2018, 2018.](#)~~Yan, Y., Lin, J., and He, C.: Ozone trends over~~  
941 ~~the United States at different times of day, *Atmos. Chem. Phys. Discuss.*,~~  
942 ~~<https://doi.org/10.5194/acp-2017-659>, in review, 2017a.~~

943 ~~Yan, Y., Pozzer, A., Ojha, N., Lin, J., and Lelieveld, J.: Analysis of European ozone~~  
944 ~~trends in the period 1995–2014, *Atmos. Chem. Phys. Discuss.*,~~  
945 ~~<https://doi.org/10.5194/acp-2017-1077>, in review, 2017b.~~

946 Yan, Y. Y., Lin, J. T., Kuang, Y., Yang, D., and Zhang, L.: Tropospheric carbon  
947 monoxide over the Pacific during HIPPO: two-way coupled simulation of GEOS-  
948 Chem and its multiple nested models, *Atmospheric Chemistry and Physics*, 14,  
949 12649-12663, 10.5194/acp-14-12649-2014, 2014.

950 Yin, X. F., Kang, S. C., de Foy, B., Cong, Z. Y., Luo, J. L., Zhang, L., Ma, Y. M.,  
951 Zhang, G. S., Rupakheti, D., and Zhang, Q. G.: Surface ozone at Nam Co in the  
952 inland Tibetan Plateau: variation, synthesis comparison and regional  
953 representativeness, *Atmospheric Chemistry and Physics*, 17, 11293-11311,  
954 10.5194/acp-17-11293-2017, 2017.

955 Young, P. J., Archibald, A. T., Bowman, K. W., Lamarque, J. F., Naik, V., Stevenson,  
956 D. S., Tilmes, S., Voulgarakis, A., Wild, O., Bergmann, D., Cameron-Smith, P.,  
957 Cionni, I., Collins, W. J., Dalsoren, S. B., Doherty, R. M., Eyring, V., Faluvegi,  
958 G., Horowitz, L. W., Josse, B., Lee, Y. H., MacKenzie, I. A., Nagashima, T.,  
959 Plummer, D. A., Righi, M., Rumbold, S. T., Skeie, R. B., Shindell, D. T., Strode,  
960 S. A., Sudo, K., Szopa, S., and Zeng, G.: Pre-industrial to end 21st century  
961 projections of tropospheric ozone from the Atmospheric Chemistry and Climate  
962 Model Intercomparison Project (ACCMIP), *Atmospheric Chemistry and Physics*,  
963 13, 2063-2090, 10.5194/acp-13-2063-2013, 2013.

964 Zhang, L., Jacob, D. J., Boersma, K. F., Jaffe, D. A., Olson, J. R., Bowman, K. W.,  
965 Worden, J. R., Thompson, A. M., Avery, M. A., Cohen, R. C., Dibb, J. E., Flock,  
966 F. M., Fuelberg, H. E., Huey, L. G., McMillan, W. W., Singh, H. B., and  
967 Weinheimer, A. J.: Transpacific transport of ozone pollution and the effect of  
968 recent Asian emission increases on air quality in North America: an integrated

969 analysis using satellite, aircraft, ozonesonde, and surface observations,  
970 *Atmospheric Chemistry and Physics*, 8, 6117-6136, 2008.

971 Zhang, Q., Streets, D. G., Carmichael, G. R., He, K. B., Huo, H., Kannari, A.,  
972 Klimont, Z., Park, I. S., Reddy, S., Fu, J. S., Chen, D., Duan, L., Lei, Y., Wang,  
973 L. T., and Yao, Z. L.: Asian emissions in 2006 for the NASA INTEX-B mission,  
974 *Atmos. Chem. Phys.*, 9, 5131–5153, doi:10.5194/acp-9-5131-2009, 2009.

975 Zhang, Q., Jiang, X. J., Tong, D., Davis, S. J., Zhao, H. Y., Geng, G. N., Feng, T.,  
976 Zheng, B., Lu, Z. F., Streets, D. G., Ni, R. J., Brauer, M., van Donkelaar, A.,  
977 Martin, R. V., Huo, H., Liu, Z., Pan, D., Kan, H. D., Yan, Y. Y., Lin, J. T., He, K.  
978 B., and Guan, D. B.: Transboundary health impacts of transported global air  
979 pollution and international trade, *Nature*, 543, 705-709, 10.1038/nature21712,  
980 2017.

981 Zhao, B., Wang, S. X., Liu, H., Xu, J. Y., Fu, K., Klimont, Z., Hao, J. M., He, K. B.,  
982 Cofala, J., and Amann, M.: NO<sub>x</sub> emissions in China: historical trends and future  
983 perspectives, *Atmos. Chem. Phys.*, 13, 9869-9897, 10.5194/acp-13-9869-2013,  
984 2013.

985 Zhu, B., Hou, X. W., and Kang, H. Q.: Analysis of the seasonal ozone budget and the  
986 impact of the summer monsoon on the northeastern Qinghai-Tibetan Plateau, *J.*  
987 *Geophys. Res.-Atmos.*, 121, 2029-2042, 10.1002/2015jd023857, 2016.

988

989

990 Table 1. Emissions used in the model.

Region	Inventory	Resolution <sup>a</sup>	Year	Species <sup>b</sup>	References & Notes
Anthropogenic emissions					
Global	EDGAR v4.2	0.1° x 0.1°, monthly	2008	NOx, SO2, CO, NH3	<a href="http://edgar.jrc.ec.europa.eu/overview.php?v=42">http://edgar.jrc.ec.europa.eu/overview.php?v=42</a>
Global	BOND	1° x 1°, monthly	2000	BC and OC	Bond et al. (2007)
Global	RETRO	0.5° x 0.5°, monthly	2000	NMVOC	<a href="ftp://ftp.retro.enes.org/pub/emissions/aggregated/anthro/0.5x0.5/2000/">ftp://ftp.retro.enes.org/pub/emissions/aggregated/anthro/0.5x0.5/2000/</a>
Global	ICOADS, shipping	1° x 1°, monthly	2002	NOx, SO2, CO	Wang et al. (2008); <a href="http://coast.cms.udel.edu/GlobalShipEmissions/">http://coast.cms.udel.edu/GlobalShipEmissions/</a>
Global	AEIC, aircraft	1° x 1°, annual	2005	NOx, SO2, CO, NMVOC, BC, OC	Simone et al. (2013)
Asia	INTEX-B	1° x 1°, monthly	2006	NOx, SO2, CO, NMVOC, BC, OC, NH3	Zhang et al. (2009). NH3 only available for 2000.
China	MEIC	0.25° x 0.25°, monthly	2008	NOx, SO2, CO, NMVOC, NH3	Li et al. (2017); Geng et al. (2017); <a href="http://www.meicmodel.org/">http://www.meicmodel.org/</a> .
United States	NEI2005	4km x 4km, monthly & weekend/weekday	2005 <sup>c</sup>	NOx, SO2, CO, NMVOC, NH3, BC, OC	<a href="ftp://aftp.fsl.noaa.gov/divisions/taq/emissions_data_2005">ftp://aftp.fsl.noaa.gov/divisions/taq/emissions_data_2005</a>
Canada	CAC	1° x 1°, annual	2008	NOx, SO2, CO, NH3	<a href="http://www.ec.gc.ca/pdb/cac/cac_home_e.cfm">http://www.ec.gc.ca/pdb/cac/cac_home_e.cfm</a>
Mexico	BRAVO	1° x 1°, annual	1999 <sup>c</sup>	NOx, SO2, CO	Kuhns et al. (2005)
Europe	EMEP	1° x 1°, monthly	2007	NOx, SO2, CO	Auvray and Bey (2005); <a href="http://www.emep.int/index.html">http://www.emep.int/index.html</a>
Biomass burning emissions					
Global	GFED3	0.5° x 0.5°, daily	2008	NOx, SO2, CO, NMVOC, NH3, BC, OC	van der Werf et al., 2010; <a href="http://www.globalfiredata.org">http://www.globalfiredata.org</a>
Natural/Semi-natural emissions (online calculation)					
Global	MEGAN v2.1	Model resolution	2008	ISOP, monoterpenes, sesquiterpenes, MOH, ACET, ETOH, CH2O, ALD2, HCOOH, C2H4, TOLU, PRPE	Guenther et al. (2012)
Global	Soil NOx	Model resolution	2008	NO	Hudman et al. (2012)
Global	Lightning NOx	Model resolution	2008	NO	Murray et al. (2012)

991 a. Before re-gridded to model horizontal resolutions. For more information, see  
992 [http://wiki.seas.harvard.edu/geos-chem/index.php/Anthropogenic\\_emissions](http://wiki.seas.harvard.edu/geos-chem/index.php/Anthropogenic_emissions).

993 b. Notes for NMVOC: RETRO includes PRPE, C3H8, ALK4, ALD2, CH2O and  
994 MEK; in the CTM, MEK emissions are further allocated to MEK (25%) and ACET  
995 (75%). AEIC, INTEX-B and MEIC include PRPE, C2H6, C3H8, ALK4, ALD2,  
996 CH2O, MEK and ACET. NEI05 includes PRPE, C3H8, ALK4, CH2O, MEK and

997 ACET. EMEP includes PRPE, ALK4, ALD2 and MEK. Emissions of C<sub>2</sub>H<sub>6</sub> outside  
998 Asia are from Xiao et al. (2008).

999 c. Over the United States and Mexico, emissions of CO, NO<sub>x</sub> are scaled to 2008 and  
1000 2006 respectively. ([http://wiki.seas.harvard.edu/geos-  
1001 chem/index.php/Scale\\_factors\\_for\\_anthropogenic\\_emissions](http://wiki.seas.harvard.edu/geos-chem/index.php/Scale_factors_for_anthropogenic_emissions)).

1002 Table 2. Model simulations.

Full chemistry simulation	Description	Tagged ozone simulation	Description
CTL	Full-chemistry simulation with all emissions	T_CTL	Driven by daily ozone production and loss rate archived from CTL
xANTH	Without global anthropogenic emissions	T_xANTH	With respect to xANTH
xCH	Without anthropogenic emissions of China	T_xCH	With respect to xCH
xJAKO	Without anthropogenic emissions of Japan and Korea	T_xJAKO	With respect to xJAKO
xSEA	Without anthropogenic emissions of South-East Asia	T_xSEA	With respect to xSEA
xSA	Without anthropogenic emissions of South Asia	T_xSA	With respect to xSA
xROA	Without anthropogenic emissions of Rest of Asia	T_xROA	With respect to xROA
xEU	Without anthropogenic emissions of Europe	T_xEU	With respect to xEU
xNA	Without anthropogenic emissions of North America	T_xNA	With respect to xNA
xROW	Without anthropogenic emissions of Rest of World	T_xROW	With respect to xROW

1003

1004 Table 3. Comparison of simulated and observed springtime MDA8 ozone and CO at  
 1005 five regional background sites in China and six global background stations nearby  
 1006 China with hourly measurements.

Country	Site	Location	Year	MDA8-Ozone			CO		
				Obs	Model	NMB	Obs	Model	NMB
				(ppb)	(ppb)	(%)	(ppb)	(ppb)	(%)
China	Gucheng	39.1°N, 115.7°E, 15m	2007	48.8	50.2	2.9			
	Longfengshan	44.7°N, 127.6°E, 331m	2007	50.6	52.9	4.5	290	251	-13.4
	Lin'an	30.2°N, 119.7°E, 132m	2008	65.1	68.9	5.8	628	418	-33.4
	Shangri-La	28.0°N, 99.4°E, 3580m	2008	61.4	68.7	11.9	181	139	-23.2
	Waliguan	36.3°N, 100.9°E, 3816m	2008	56.5	64.4	14.0			
Kyrgyzstan	Issyk-Kul	42.6°N, 77.0°E, 1640m	2008	52.8	59.0	11.7			
Nepal	Everest-Pyramid	28.0°N, 86.8°E, 5079m	2008	66.3	79.1	19.3			
Indonesia	Bukit-Koto-Tabang	0.2°S, 100.3°E, 865m	2008				141	146	3.5
Japan	Yonagunijima	24.5°N, 123.0°E, 30m	2008	54.8	56.4	2.9	208	157	-24.5
	Tsukuba	36.1°N, 140.1°E, 25m	2008	47.2	56.0	18.6			
	Ryori	39.0°N, 141.8°E, 260m	2008	54.6	54.7	0.2	211	203	-3.8

1007

1008

Country	Site	Location	Year	MDA8 ozone			CO			References & Notes
				Obs	Model	NMB	Obs	Model	NMB	
				(ppb)	(ppb)	(%)	(ppb)	(ppb)	(%)	
China	Gucheng	39.1°N, 115.7°E, 15m	2007	48.8	50.2	2.9				Lin et al., 2009
	Longfengshan	44.7°N, 127.6°E, 331m	2007	50.6	52.9	4.5	290	251	-13.4	
	Lin'an	30.2°N, 119.7°E, 132m	2008	65.1	68.9	5.8	628	418	-33.4	Xu et al., 2008
	Shangri-La	28.0°N, 99.4°E, 3580m	2008	61.4	68.7	11.9	181	139	-23.2	Ma et al., 2014

	<u>Waliguan</u>	<u>36.3°N, 100.9°E, 3816m</u>	<u>2008</u>	<u>56.5</u>	<u>64.4</u>	<u>14.0</u>				<u>Xu et al., 2016</u>
<u>Kyrgyzstan</u>	<u>Issyk-Kul</u>	<u>42.6°N, 77.0°E, 1640m</u>	<u>2008</u>	<u>52.8</u>	<u>59.0</u>	<u>11.7</u>				
<u>Nepal</u>	<u>Everest-Pyramid</u>	<u>28.0°N, 86.8°E, 5079m</u>	<u>2008</u>	<u>66.3</u>	<u>79.1</u>	<u>19.3</u>				
<u>Indonesia</u>	<u>Bukit Koto Tabang</u>	<u>0.2°S, 100.3°E, 865m</u>	<u>2008</u>				<u>141</u>	<u>146</u>	<u>3.5</u>	<a href="http://ds.data.jma.go.jp/gmd/wdcgg/cgi-bin/wdcgg/catalogue.cgi">http://ds.data.jma.go.jp/gmd/wdcgg/cgi-bin/wdcgg/catalogue.cgi</a>
	<u>Yonagunijima</u>	<u>24.5°N, 123.0°E, 30m</u>	<u>2008</u>	<u>54.8</u>	<u>56.4</u>	<u>2.9</u>	<u>208</u>	<u>157</u>	<u>-24.5</u>	
<u>Japan</u>	<u>Tsukuba</u>	<u>36.1°N, 140.1°E, 25m</u>	<u>2008</u>	<u>47.2</u>	<u>56.0</u>	<u>18.6</u>				
	<u>Ryori</u>	<u>39.0°N, 141.8°E, 260m</u>	<u>2008</u>	<u>54.6</u>	<u>54.7</u>	<u>0.2</u>	<u>211</u>	<u>203</u>	<u>-3.8</u>	

1009

1010 Table 4. Comparison of simulated springtime monthly mean ozone with observations  
 1011 from EANET and literature.

Country	Site	Year	Location	Characteristics	Obs (ppb)	Model (ppb)	NMB (%)
Japan (EANET)	Rishiri	2008	45.5°N, 141.2°E, 40m	Remote	55.0	46.0	-16.5
	Ochiishi	2008	43.1°N, 145.5°E, 49m	Remote	48.4	46.7	-3.6
	Tappi	2008	41.3°N, 140.4°E, 105m	Remote	66.2	48.8	-26.2
	Sado-seki	2008	38.2°N, 138.4°E, 136m	Remote	61.3	53.3	-13.0
	Happo	2008	36.7°N, 137.8°E, 1850m	Remote	62.0	53.8	-13.2
	Ijira	2008	35.6°N, 136.7°E, 140m	Rural	30.7	47.8	55.7
	Oki	2008	36.3°N, 133.2°E, 90m	Remote	58.8	55.7	-5.3
	Banryu	2008	34.7°N, 131.8°E, 53m	Urban	48.5	52.1	7.5
	Yusuhara	2008	33.4°N, 132.9°E, 790m	Remote	53.7	53.1	-1.1
	Hedo	2008	26.9°N, 128.3°E, 60m	Remote	53.6	54.2	1.1
Republic of Korea (EANET)	Ogasawara	2008	27.1°N, 142.2°E, 230m	Remote	37.9	41.1	8.3
	Kanghwa	2008	37.7°N, 126.3°E, 150m	Rural	52.3	47.4	-9.4
	Cheju	2008	33.3°N, 126.2°E, 72m	Remote	56.3	57.7	2.5
Russia (EANET)	Imsil	2008	35.6°N, 127.2°E	Rural	30.3	48.2	58.8
China (literature)	Mondy	2008	51.7°N, 101.0°E, 2000m	Remote	43.0	49.2	14.4
	Miyun	2006	40.5°N, 116.8°E, 152m	Rural	48.7	35.3	-27.4
	Mt. Tai	2004-2005	24.25°N, 117.10°E, 1533m	Rural	57.0	54.8	-3.9
	Mt. Hua	2004-2005	34.49°N, 110.09°E, 2064m	Rural	50.0	51.8	3.5
	Mt. Huang	2004-2005	30.13°N, 118.15°E, 1836m	Rural	59.3	54.0	-9.0
	Hok Tsui, HongKong	1994-2007	22.2°N, 114.2°E, 60m	Rural	36.0	53.4	48.2
	Nanjing	2000-2002	32.1°N, 118.7°E	Urban	27.0	31.3	16.0

1012

1013

Country	Site	Year	Location	Characteristics	Obs (ppb)	Model (ppb)	NMB (%)	References & Notes
Japan (EANET)	<u>Rishiri</u>	<u>2008</u>	<u>45.5°N, 141.2°E, 40m</u>	<u>Remote</u>	<u>55.0</u>	<u>46.0</u>	<u>-16.5</u>	<a href="http://www.eanet.asia/product/index.html">http://www.eanet.asia/product/index.html</a>
	<u>Ochiishi</u>	<u>2008</u>	<u>43.1°N, 145.5°E, 49m</u>	<u>Remote</u>	<u>48.4</u>	<u>46.7</u>	<u>-3.6</u>	
	<u>Tappi</u>	<u>2008</u>	<u>41.3°N, 140.4°E, 105m</u>	<u>Remote</u>	<u>66.2</u>	<u>48.8</u>	<u>-26.2</u>	
	<u>Sado-seki</u>	<u>2008</u>	<u>38.2°N, 138.4°E, 136m</u>	<u>Remote</u>	<u>61.3</u>	<u>53.3</u>	<u>-13.0</u>	
	<u>Happo</u>	<u>2008</u>	<u>36.7°N, 137.8°E, 1850m</u>	<u>Remote</u>	<u>62.0</u>	<u>53.8</u>	<u>-13.2</u>	
	<u>Ijira</u>	<u>2008</u>	<u>35.6°N, 136.7°E, 140m</u>	<u>Rural</u>	<u>30.7</u>	<u>47.8</u>	<u>55.7</u>	
	<u>Oki</u>	<u>2008</u>	<u>36.3°N, 133.2°E, 90m</u>	<u>Remote</u>	<u>58.8</u>	<u>55.7</u>	<u>-5.3</u>	
	<u>Banryu</u>	<u>2008</u>	<u>34.7°N, 131.8°E, 53m</u>	<u>Urban</u>	<u>48.5</u>	<u>52.1</u>	<u>7.5</u>	
	<u>Yusuhara</u>	<u>2008</u>	<u>33.4°N, 132.9°E, 790m</u>	<u>Remote</u>	<u>53.7</u>	<u>53.1</u>	<u>-1.1</u>	

	<u>Hedo</u>	<u>2008</u>	<u>26.9°N, 128.3°E, 60m</u>	<u>Remote</u>	<u>53.6</u>	<u>54.2</u>	<u>1.1</u>	
	<u>Ogasawara</u>	<u>2008</u>	<u>27.1°N, 142.2°E, 230m</u>	<u>Remote</u>	<u>37.9</u>	<u>41.1</u>	<u>8.3</u>	
<u>Republic of Korea</u> <u>(EANET)</u>	<u>Kanghwa</u>	<u>2008</u>	<u>37.7°N, 126.3°E, 150m</u>	<u>Rural</u>	<u>52.3</u>	<u>47.4</u>	<u>-9.4</u>	
	<u>Cheju</u>	<u>2008</u>	<u>33.3°N, 126.2°E, 72m</u>	<u>Remote</u>	<u>56.3</u>	<u>57.7</u>	<u>2.5</u>	
	<u>Imsil</u>	<u>2008</u>	<u>35.6°N, 127.2°E</u>	<u>Rural</u>	<u>30.3</u>	<u>48.2</u>	<u>58.8</u>	
<u>Russia (EANET)</u>	<u>Mondy</u>	<u>2008</u>	<u>51.7°N, 101.0°E, 2000m</u>	<u>Remote</u>	<u>43.0</u>	<u>49.2</u>	<u>14.4</u>	
<u>China (literature)</u>	<u>Miyun</u>	<u>2006</u>	<u>40.5°N, 116.8°E, 152m</u>	<u>Rural</u>	<u>48.7</u>	<u>35.3</u>	<u>-27.4</u>	<u>Wang et al. (2011)</u>
	<u>Mt. Tai</u>	<u>2004</u>	<u>24.25°N, 117.10°E, 1533m</u>	<u>Rural</u>	<u>57.0</u>	<u>54.8</u>	<u>-3.9</u>	
	<u>Mt. Hua</u>	<u>2004</u>	<u>34.49°N, 110.09°E, 2064m</u>	<u>Rural</u>	<u>50.0</u>	<u>51.8</u>	<u>3.5</u>	<u>Li et al. (2007)</u>
	<u>Mt. Huang</u>	<u>2004</u>	<u>30.13°N, 118.15°E, 1836m</u>	<u>Rural</u>	<u>59.3</u>	<u>54.0</u>	<u>-9.0</u>	
	<u>Hok Tsui, HongKong</u>	<u>1994-2007</u>	<u>22.2°N, 114.2°E, 60m</u>	<u>Rural</u>	<u>36.0</u>	<u>53.4</u>	<u>48.2</u>	<u>Wang et al. (2009)</u>
	<u>Nanjing</u>	<u>2000-2002</u>	<u>32.1°N, 118.7°E</u>	<u>Urban</u>	<u>27.0</u>	<u>31.3</u>	<u>16.0</u>	<u>Tu et al. (2007)</u>

1014

1015 Table 5. Springtime anthropogenic emissions of NO<sub>x</sub>, CO and NMVOC of each  
 1016 region defined in Fig. 1.

	China	Japan- and- Korea	South- East Asia	Sout h- Asia	Rest- of- Asia	Europ e	North- Americ a	Rest- of- world
NO <sub>x</sub> (TgN)	2.0	0.3	0.4	0.4	0.7	1.2	1.3	1.0
CO (Tg)	42.3	16.7	10.9	16.7	10.0	12.5	17.7	25.5
NMVOC	2.9	0.2	1.3	1.3	1.1	1.1	2.1	1.9

1017

1018 Table 5. Springtime anthropogenic emissions of NO<sub>x</sub>, CO and NMVOC in 2008 and  
 1019 2012 in each source region defined in Fig. 1.

<u>2008</u>	<u>China</u>	<u>Japan and Korea</u>	<u>South-East Asia</u>	<u>South Asia</u>	<u>Rest of Asia</u>	<u>Europe</u>	<u>North America</u>	<u>Rest of world</u>
<u>NO<sub>x</sub> (TgN)</u>	<u>2.0</u>	<u>0.3</u>	<u>0.4</u>	<u>0.4</u>	<u>0.7</u>	<u>1.2</u>	<u>1.3</u>	<u>1.0</u>
<u>CO (Tg)</u>	<u>42.3</u>	<u>1.7</u>	<u>10.9</u>	<u>16.7</u>	<u>10.0</u>	<u>12.5</u>	<u>17.7</u>	<u>25.5</u>
<u>NMVOC (TgC)</u>	<u>2.9</u>	<u>0.2</u>	<u>1.3</u>	<u>1.3</u>	<u>1.1</u>	<u>1.1</u>	<u>2.1</u>	<u>1.9</u>
<u>2012</u>								
<u>NO<sub>x</sub> (TgN)</u>	<u>2.2</u>	<u>0.3</u>	<u>0.6</u>	<u>1.3</u>	<u>1.0</u>	<u>1.0</u>	<u>1.1</u>	<u>1.5</u>
<u>CO (Tg)</u>	<u>39.2</u>	<u>2.4</u>	<u>15.4</u>	<u>21.3</u>	<u>8.9</u>	<u>7.9</u>	<u>13.1</u>	<u>38.0</u>
<u>NMVOC (TgC)</u>	<u>3.0</u>	<u>0.2</u>	<u>3.0</u>	<u>2.4</u>	<u>2.3</u>	<u>1.2</u>	<u>1.8</u>	<u>6.8</u>

1020

1021

1022

1023

1024

1025

1026

1027

1028

1029

1030

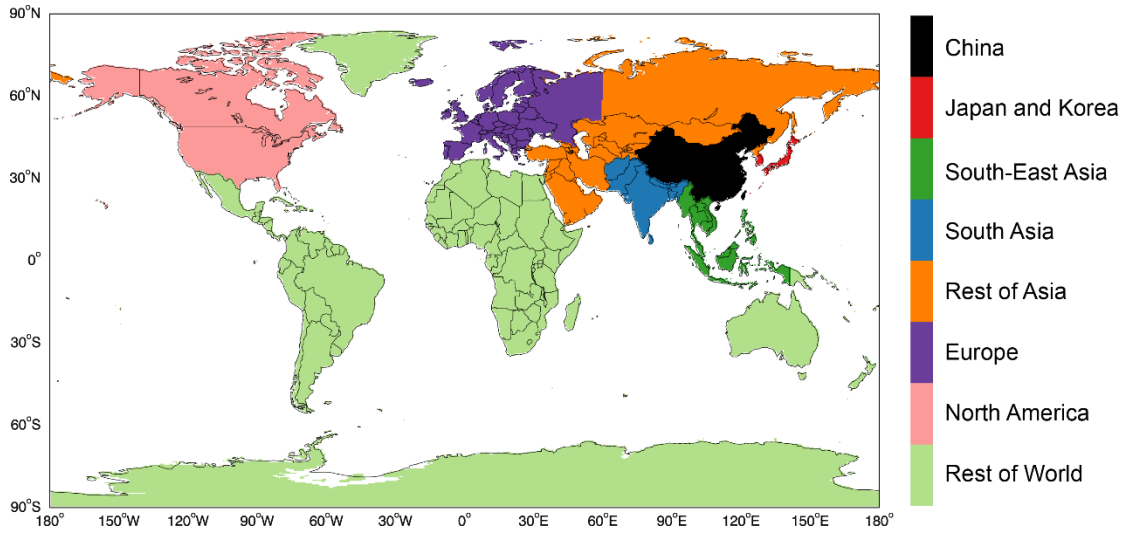
1031

1032

1033

1034

1035



1036

1037 Figure 1. Eight emission source regions.

1038

1039

1040

1041

1042

1043

1044

1045

1046

1047

1048

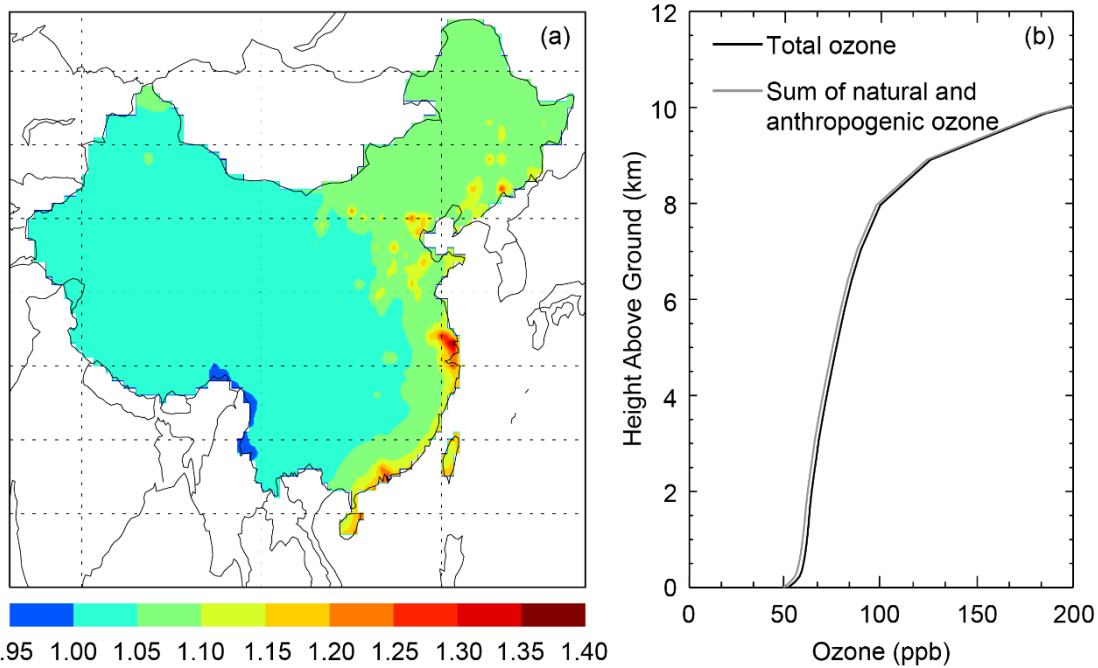
1049

1050

1051

1052

1053



1054

1055

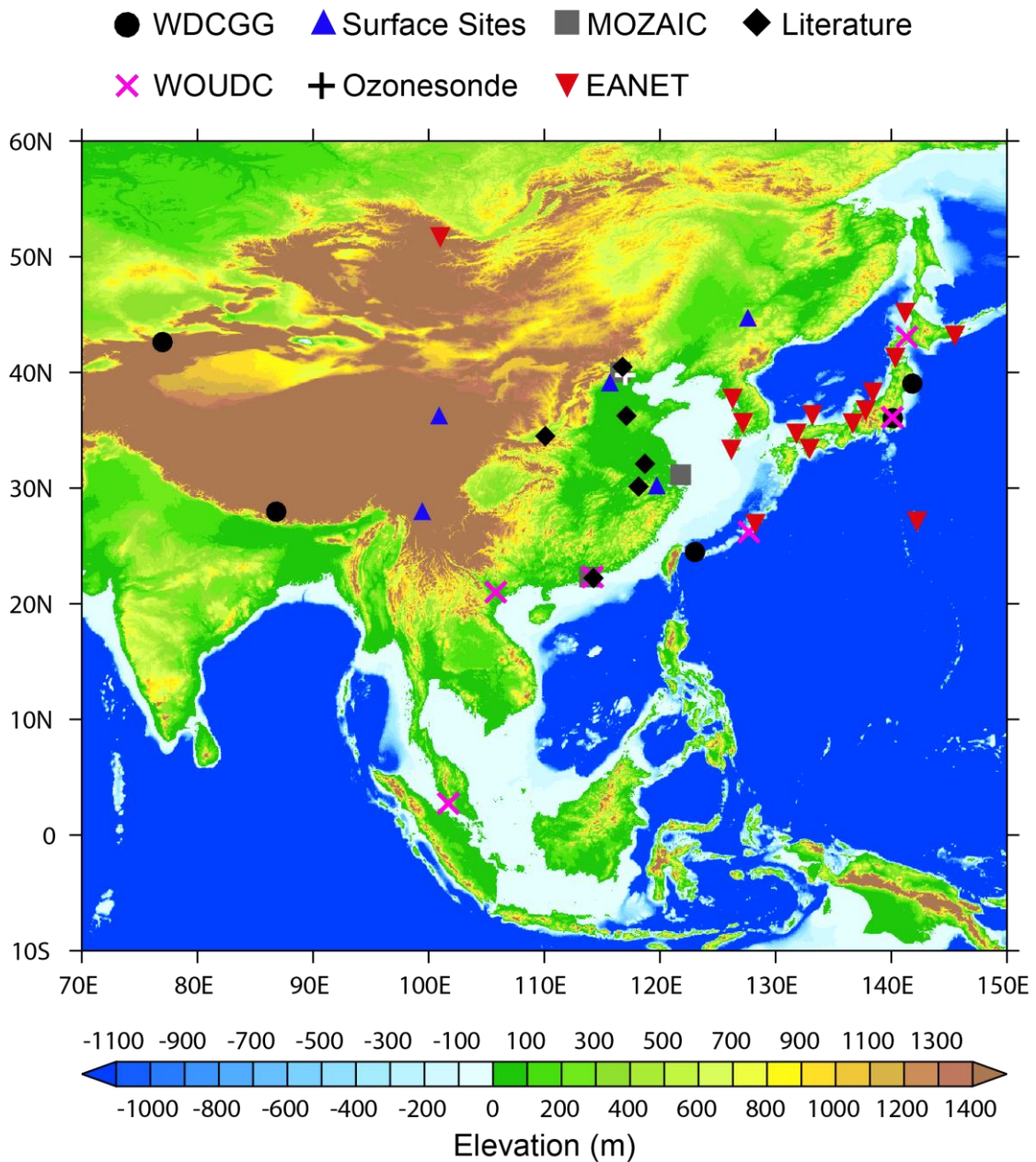
1056

1057

1058

1059

Figure 2. (a) Spatial distribution of the ratio of total surface ozone in CTL to the pre-linear-weighting-adjustment sum of natural ozone, domestic anthropogenic ozone and foreign anthropogenic ozone; (b) Vertical profile of China average total ozone in CTL and the profile of pre-linear-weighting-adjustment sum of natural ozone, domestic anthropogenic ozone and foreign anthropogenic ozone.



1060

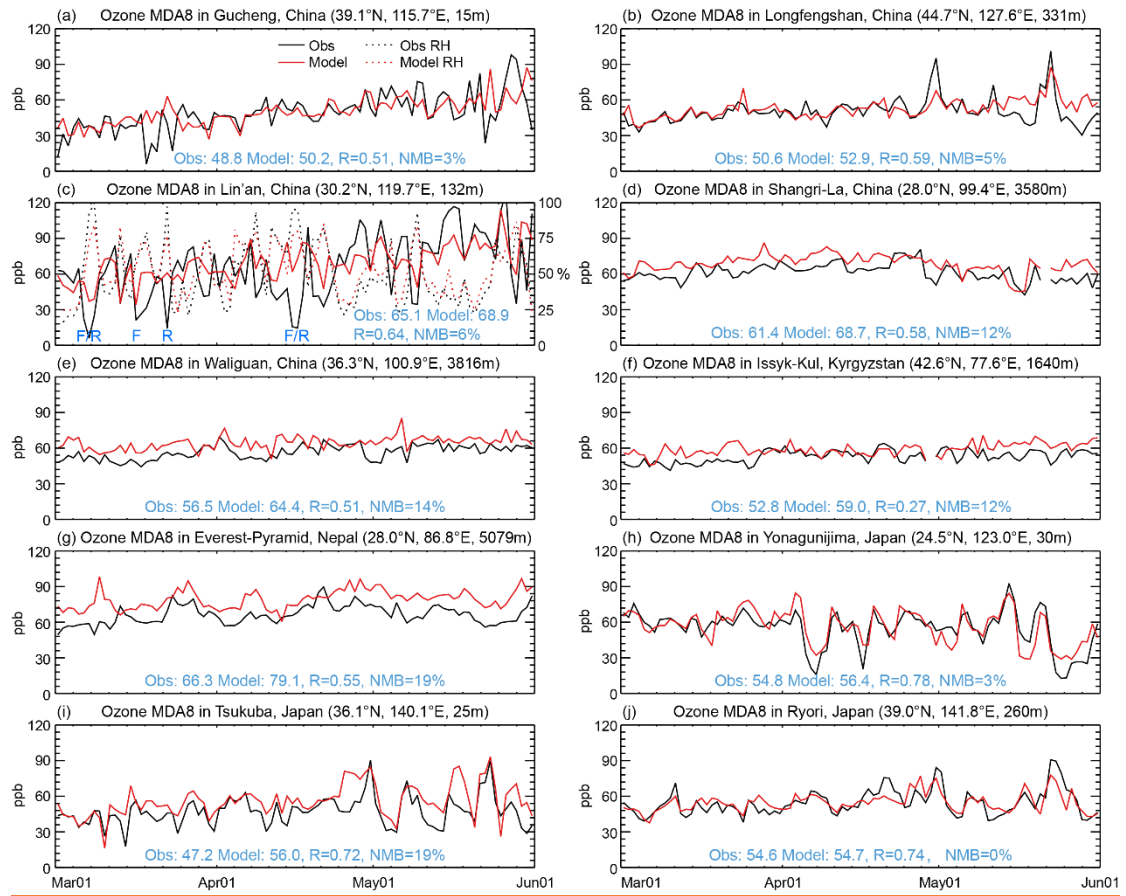
1061 Figure 23. Observation sites overlaying upon the surface elevation map from the 2  
 1062 min Gridded Global Relief Data (ETOPO2v2) available at NGDC Marine Trackline  
 1063 Geophysical database (<http://www.ngdc.noaa.gov/mgg/global/etopo2.html>).

1064

1065

1066

1067



1068

1069 Figure 34. Time series of springtime MDA8 ozone at surface sites over (a–e) China  
 1070 and (f–j) nearby countries. Due to lack of measurement data in 2008, comparisons at  
 1071 Gucheng and Longfengshan are based in 2007. In (c), observed and modeled RH are  
 1072 also compared; and the “F” and “R” symbols denote observed frog or rain,  
 1073 respectively.

1074

1075

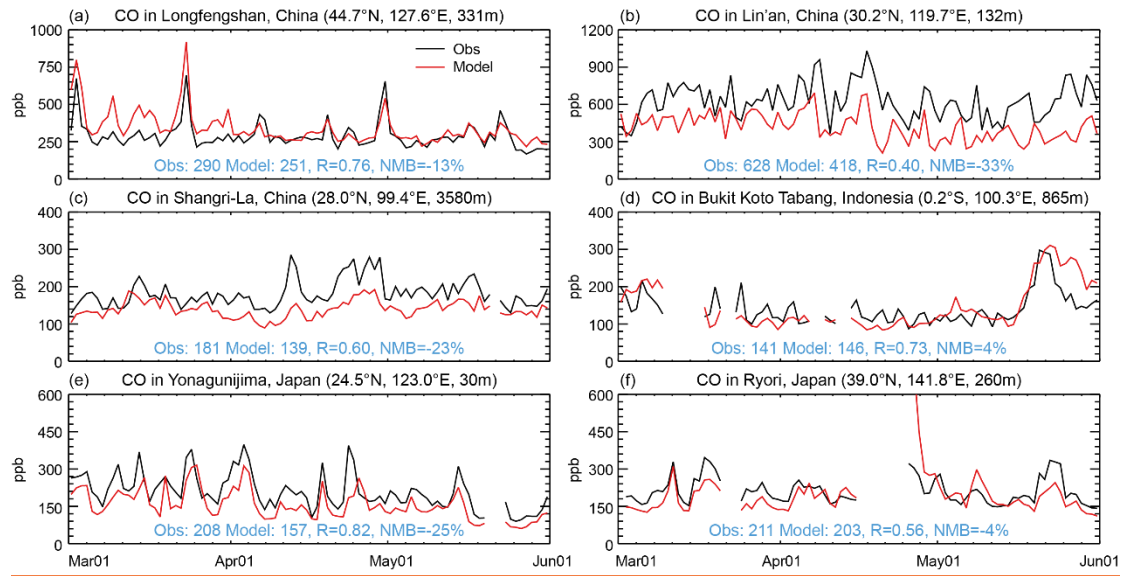
1076

1077

1078

1079

1080



1081

1082 Figure 45. Time series of daily mean CO at six surface sites over (a–c) China and (d–  
 1083 f) nearby countries.

1084

1085

1086

1087

1088

1089

1090

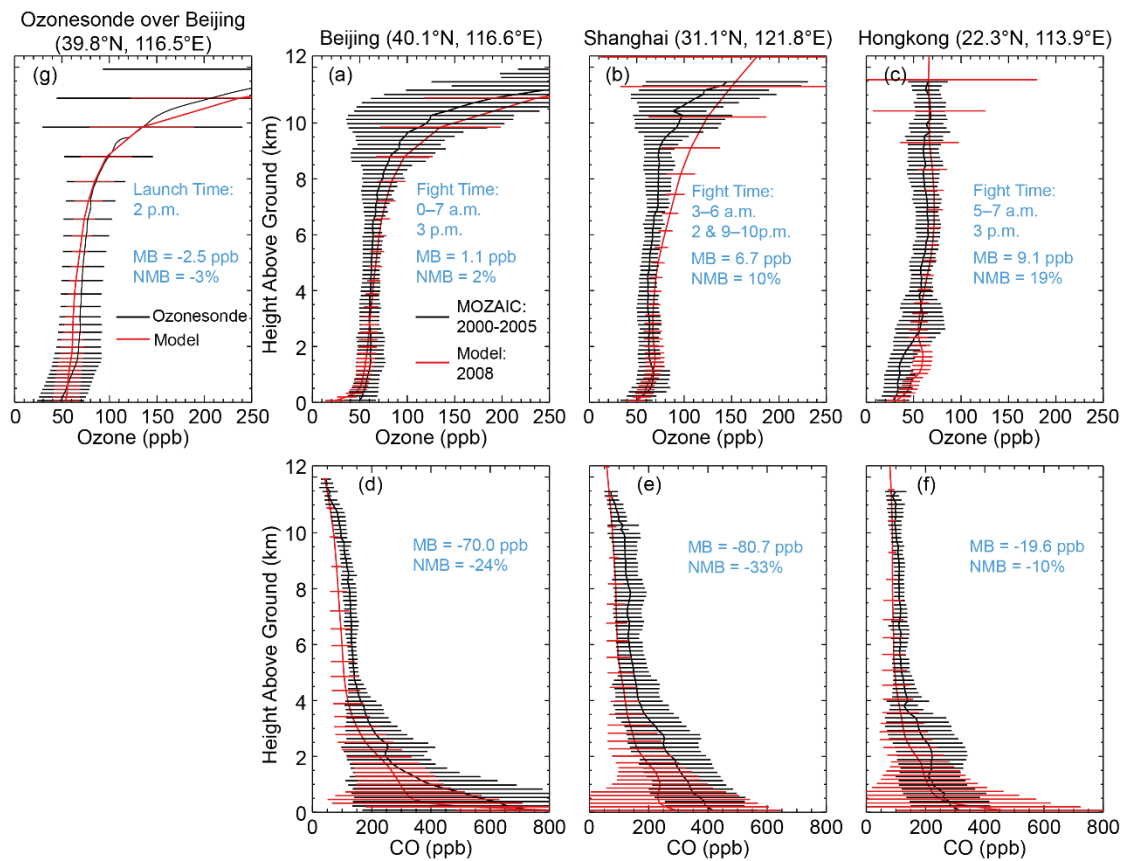
1091

1092

1093

1094

1095



1096

1097 Figure 56. Model and MOZAIC vertical profiles of (a-c) ozone and (d-f) CO over  
 1098 airports of Beijing, Shanghai and Hong Kong, averaged over multiple profiles. (g)  
 1099 Model and GPSO3 ozonesonde data over Beijing in spring 2008. Horizontal bars  
 1100 indicate ±one standard deviation across multiple profiles. Mean bias (MB),  
 1101 normalized mean bias (NMB), main flight times (local time) at each MOZAIC site and  
 1102 GPSO3 ozonesonde launch time (local time) are also shown.

1103

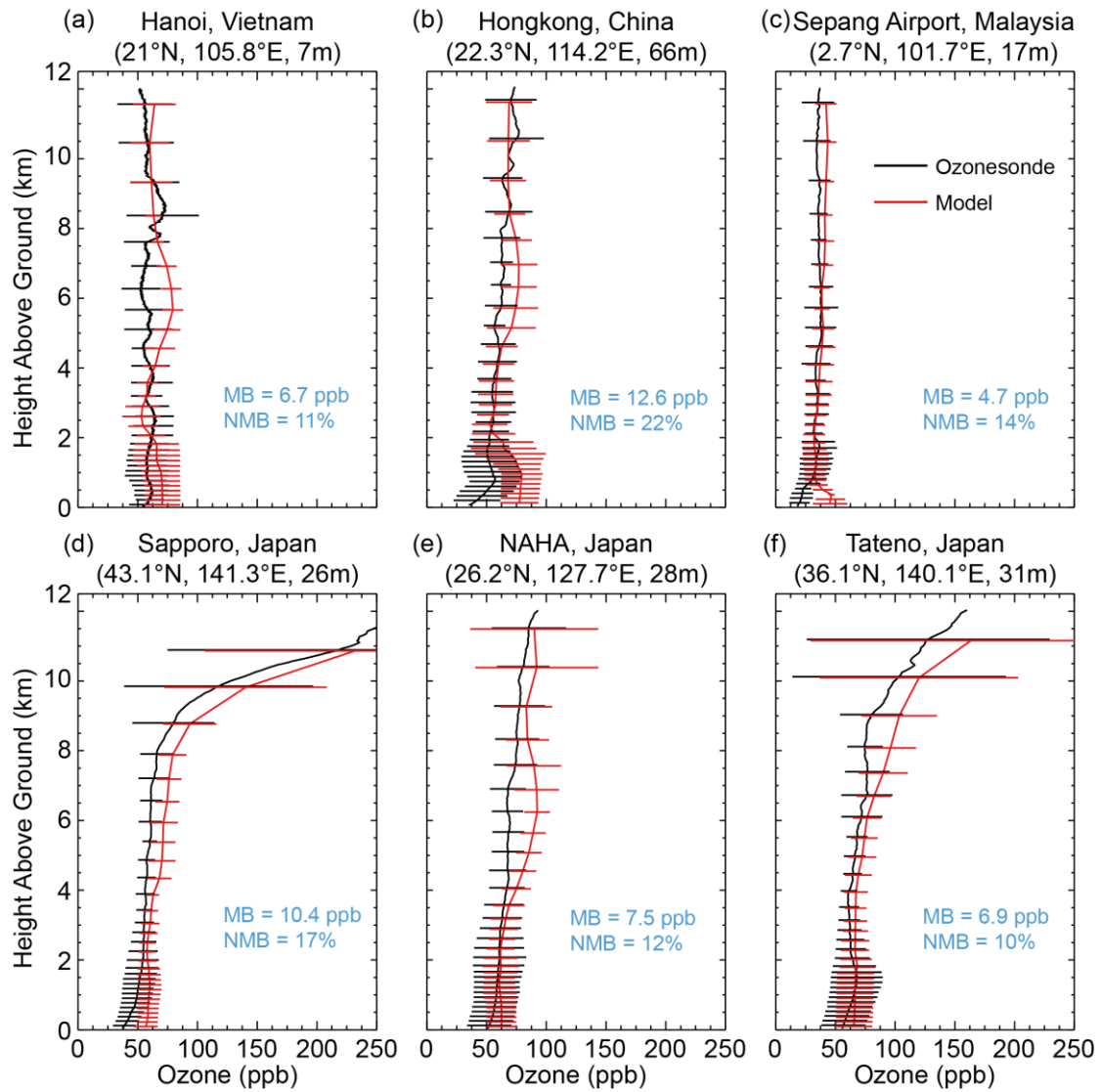
1104

1105

1106

1107

1108



1109

1110 Figure 67. Model and WOUDC ozone profiles at six sites, averaged over multiple  
 1111 profiles. Horizontal lines indicate  $\pm$ one standard deviation across multiple profiles.  
 1112 Mean bias (MB) and normalized mean bias (NMB) are shown in blue.

1113

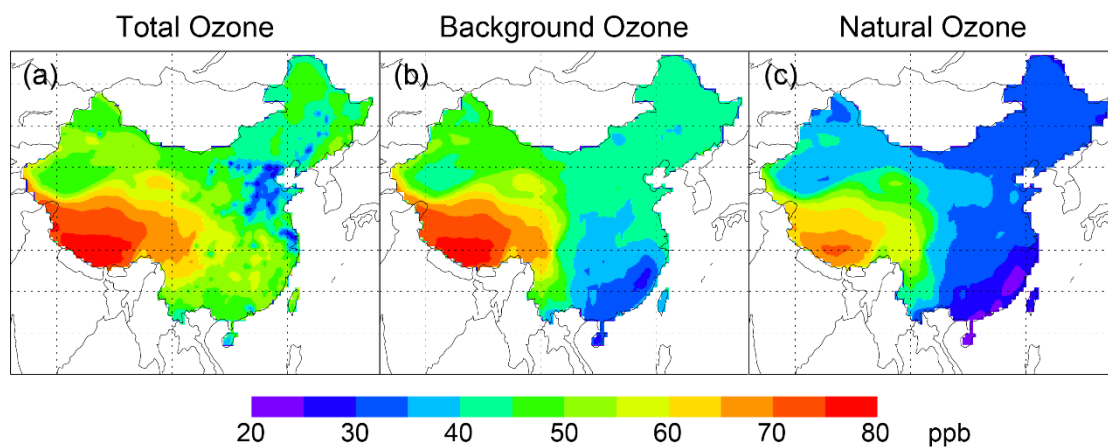
1114

1115

1116

1117

1118



1119

1120 Figure 78. Spatial distribution of springtime daily mean (a) total surface ozone, (b)  
 1121 background ozone and (c) natural ozone over China.

1122

1123

1124

1125

1126

1127

1128

1129

1130

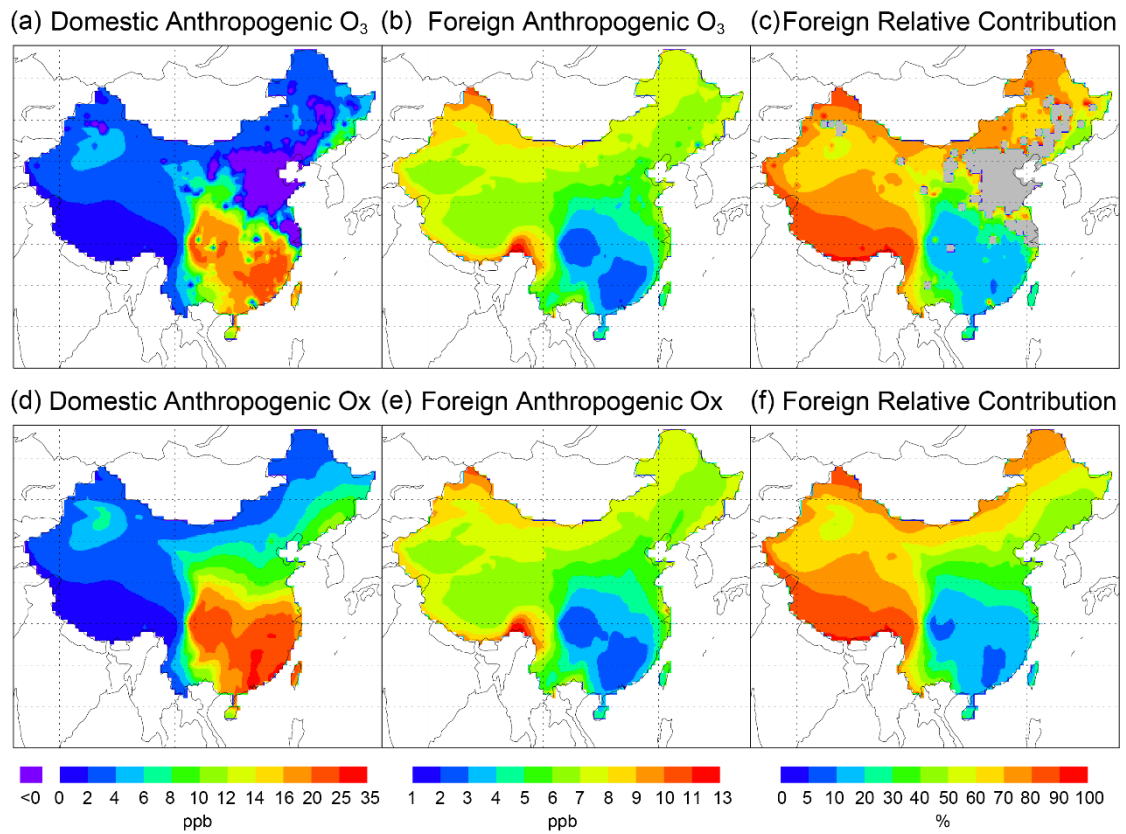
1131

1132

1133

1134

1135



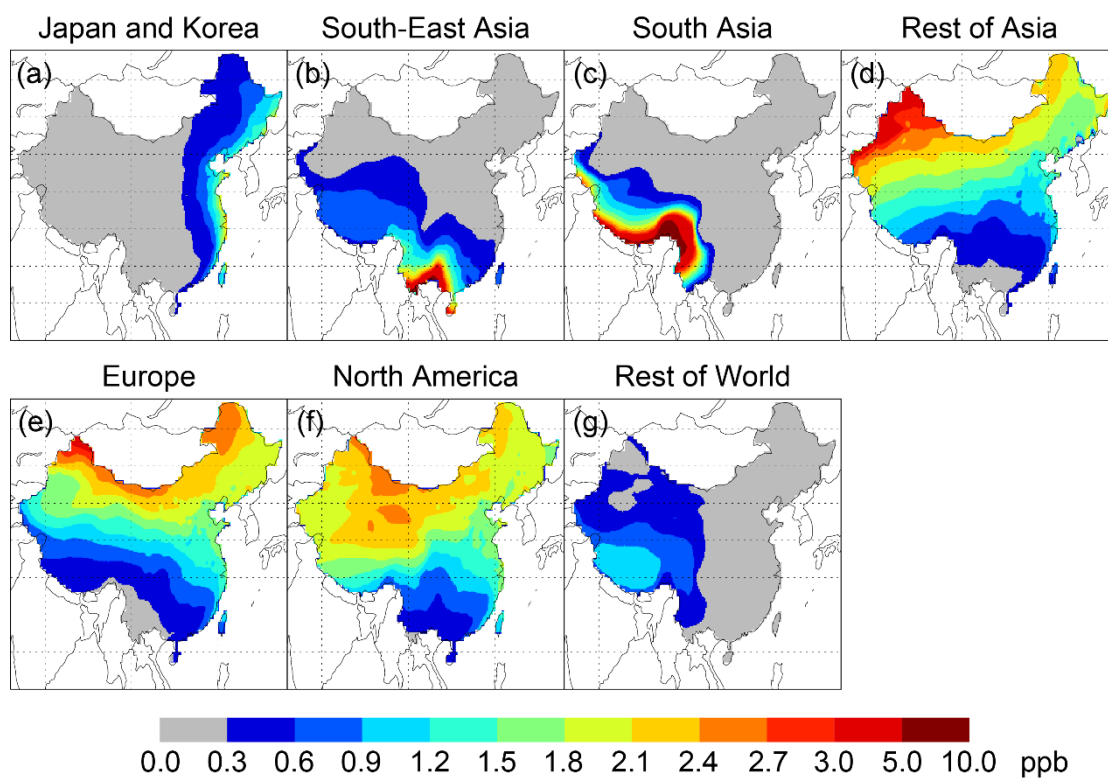
1136

1137 Figure 89. Spatial distribution of springtime daily mean surface ozone over China  
 1138 contributed by (a) domestic and (b) foreign anthropogenic emissions. (c) Percentage  
 1139 contribution of foreign anthropogenic emissions to total anthropogenic ozone; areas  
 1140 with negative Chinese contributions (due to  $NO_x$  titration) are marked in grey. (d–f)  
 1141 sSimilar to (a–c) but for  $O_x (= O_3 + NO_2)$ . The linear weighting adjustment is applied  
 1142 to derive all results. Note that the color scales are different between (a, d) and (b, e).

1143

1144

1145



1146

1147 Figure 910. Spatial distribution of springtime daily mean surface ozone over China  
 1148 contributed by anthropogenic emissions of individual regions. The ozone  
 1149 enhancement over China by anthropogenic emissions of each region is determined by  
 1150 difference between the base case simulation CTL and zero-out simulation without that  
 1151 region's anthropogenic emissions, followed by the linear weighting adjustment.

1152

1153

1154

1155

1156

1157

1158

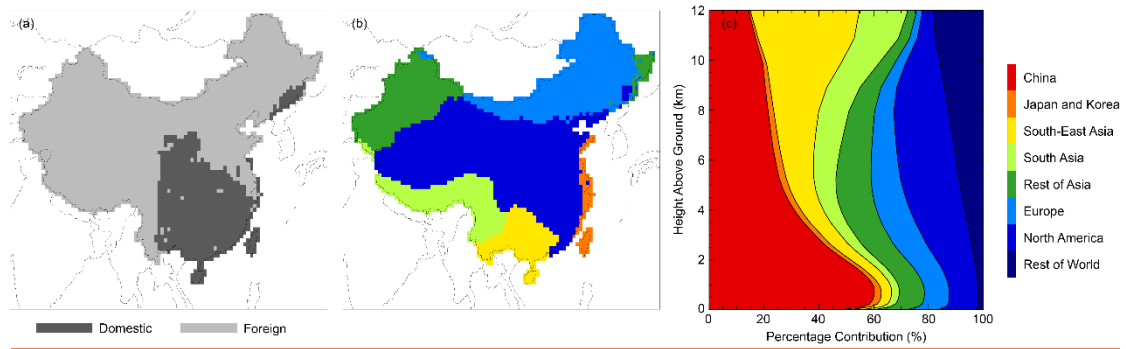
1159

1160

1161

1162

1163



1164

1165 Figure 1011. (a) Indication of the largest anthropogenic contributor (domestic or  
1166 foreign) to surface ozone at individual locations of China. (b) Indication of the largest  
1167 foreign anthropogenic contributor to surface ozone at individual locations of China.  
1168 (c) Vertical distribution of percentage contribution of each region to total  
1169 anthropogenic ozone over China.

1170

1171

1172

1173

1174

1175

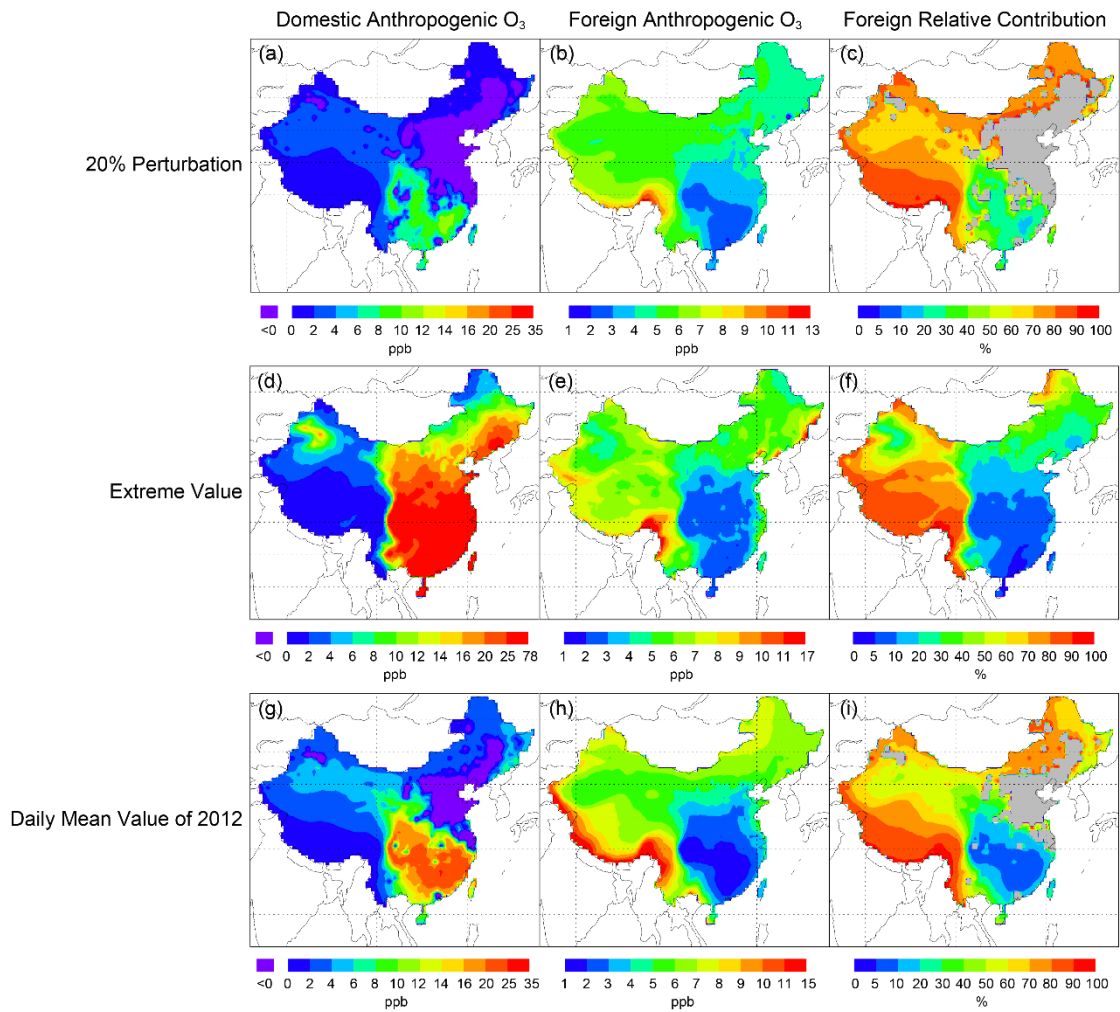
1176

1177

1178

1179

1180



1181

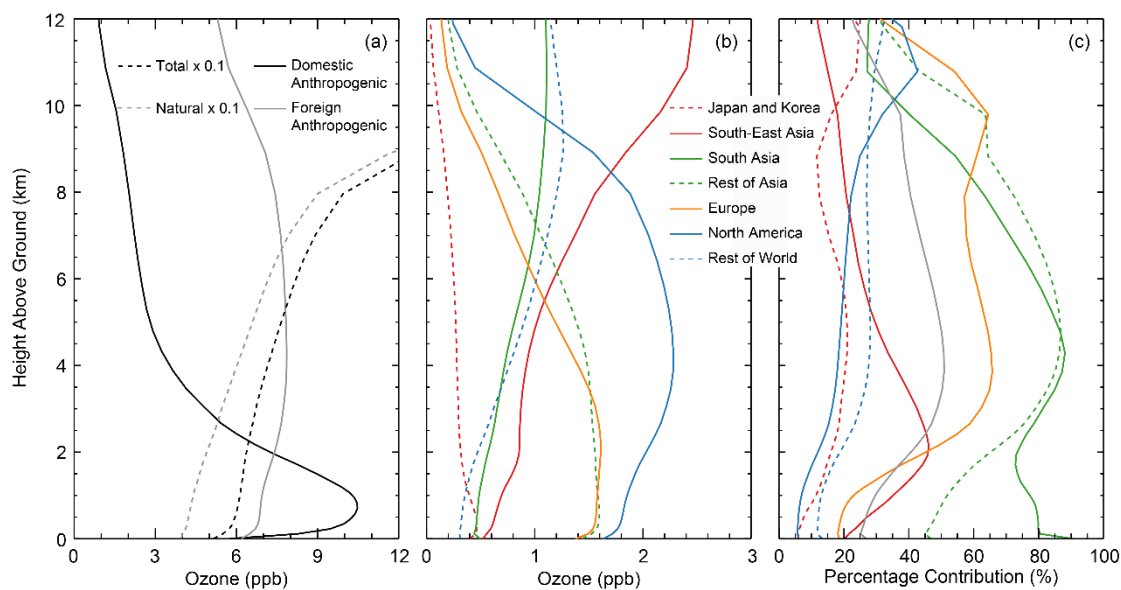
1182 Figure 12. (a–c) similar to Fig. 9a–c but for springtime daily mean ozone calculated  
 1183 by 20% perturbation method. (d–f) similar to Fig. 9a–c but for springtime extreme  
 1184 ozone value (defined as the average of the top 5% hourly ozone concentrations). (d–f)  
 1185 similar to Fig. 9a–c but for springtime daily mean ozone in 2012. The linear  
 1186 weighting adjustment is applied to derive all results. Note that the color scales are  
 1187 different in each panel.

1188

1189

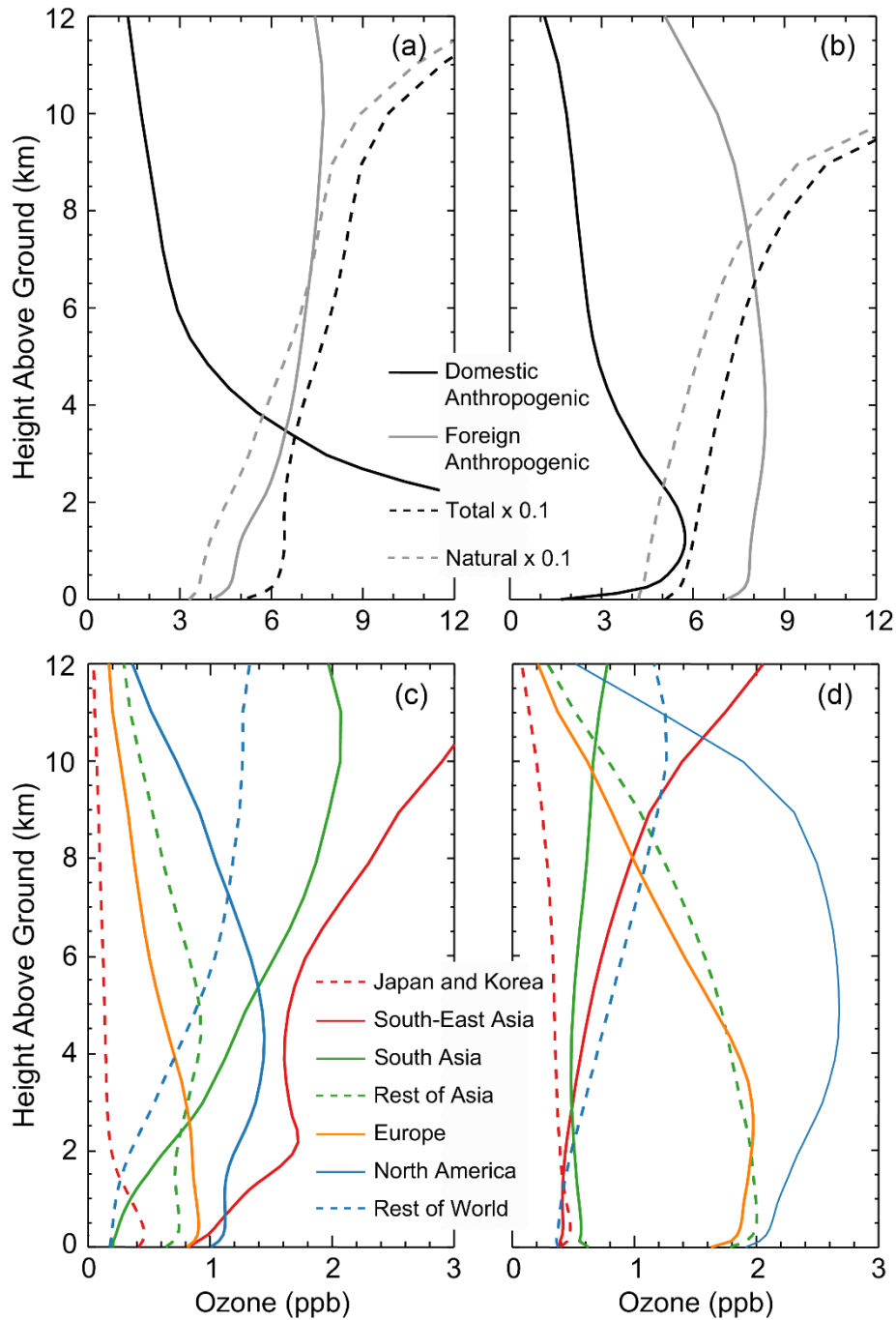
1190

1191



1192

1193 Figure 4-13. (a) Vertical distribution of China average daily mean ozone contributed  
1194 by domestic anthropogenic emissions, foreign anthropogenic emissions, and natural  
1195 sources (scaled by 0.1) and total sources (scaled by 0.1). (b) Contribution by  
1196 anthropogenic emissions of each foreign source region. (c) Of the ozone over China  
1197 due to anthropogenic emissions of each foreign region, the portion produced within  
1198 each foreign source region's territory calculated based on a combination of zero-out  
1199 and tagged simulations. The linear weighting adjustment is applied to derive all  
1200 results.



1201  
 1202  
 1203  
 1204  
 1205  
 1206  
 1207  
 1208  
 1209  
 1210  
 1211

Figure 14. (a) Vertical distribution of regional average daily mean ozone contributed by domestic anthropogenic emissions, foreign anthropogenic emissions, natural sources (scaled by 0.1) and total sources (scaled by 0.1) over regions where Chinese anthropogenic emissions contribute more surface ozone than total foreign anthropogenic emissions. (c) Contribution by anthropogenic emissions of each foreign source region over regions where Chinese anthropogenic emissions contribute more surface ozone than total foreign anthropogenic emissions. (b, d) similar to (a, c) but for regional average daily mean ozone over regions where foreign anthropogenic emissions dominate. The linear weighting adjustment is applied to derive all results.